Research Paper

GEOSPHERE

GEOSPHERE; v. 14, no. 2

doi:10.1130/GES01485.1

12 figures; 3 tables; 3 supplemental files

CORRESPONDENCE: mpecha@email.arizona.edu

CITATION: Pecha, M.E., Gehrels, G.E., Karlstrom, K.E., Dickinson, W.R., Donahue, M.S., Gonzales, D.A., and Blum, M.D., 2018, Provenance of Cretaceous through Eocene strata of the Four Corners region: Insights from detrital zircons in the San Juan Basin, New Mexico and Colorado: Geosphere, v. 14, no. 2, p. 785–811, doi:10.1130/GES01485.1.

Science Editor: Shanaka de Silva
Associate Editor: Graham D.M. Andrews

Received 11 December 2016
Revision received 9 September 2017
Accepted 5 January 2018
Published online 16 February 2018

Provenance of Cretaceous through Eocene strata of the Four Corners region: Insights from detrital zircons in the San Juan Basin, New Mexico and Colorado

Mark E. Pecha[1], George E. Gehrels[1], Karl E. Karlstrom[2], William R. Dickinson[1,†], Magdalena S. Donahue[2], David A. Gonzales[3], and Michael D. Blum[4]

[1]Department of Geosciences, University of Arizona, Tucson, Arizona 85721, USA
[2]Department of Earth and Planetary Sciences, Northrop Hall, University of New Mexico, Albuquerque, New Mexico 87131, USA
[3]Department of Geosciences, Fort Lewis College, 1000 Rim Drive, Durango, Colorado 81301, USA
[4]Department of Geology, University of Kansas, Lindley Hall, 1475 Jayhawk Boulevard, Room 120, Lawrence, Kansas 66045, USA

ABSTRACT

Cretaceous through Eocene strata of the Four Corners region provide an excellent record of changes in sediment provenance from Sevier thin-skinned thrusting through the formation of Laramide block uplifts and intra-foreland basins. During the ca. 125–50 Ma timespan, the San Juan Basin was flanked by the Sevier thrust belt to the west, the Mogollon highlands rift shoulder to the southwest, and was influenced by (ca. 75–50 Ma) Laramide tectonism, ultimately preserving a >6000 ft (>2000 m) sequence of continental, marginal-marine, and offshore marine sediments. In order to decipher the influences of these tectonic features on sediment delivery to the area, we evaluated 3228 U-Pb laser analyses from 32 detrital-zircon samples from across the entire San Juan Basin, of which 1520 analyses from 16 samples are newly reported herein. The detrital-zircon results indicate four stratigraphic intervals with internally consistent age peaks: (1) Lower Cretaceous Burro Canyon Formation, (2) Turonian (93.9–89.8 Ma) Gallup Sandstone through Campanian (83.6–72.1 Ma) Lewis Shale, (3) Campanian Pictured Cliffs Sandstone through Campanian Fruitland Formation, and (4) Campanian Kirtland Sandstone through Lower Eocene (56.0–47.8 Ma) San Jose Formation. Statistical analysis of the detrital-zircon results, in conjunction with paleocurrent data, reveals three distinct changes in sediment provenance. The first transition, between the Burro Canyon Formation and the Gallup Sandstone, reflects a change from predominantly reworked sediment from the Sevier thrust front, including uplifted Paleozoic sediments and Mesozoic eolian sandstones, to a mixed signature indicating both Sevier and Mogollon derivation. Deposition of the Pictured Cliffs Sandstone at ca. 75 Ma marks the beginning of the second transition and is indicated by the spate of near-depositional-age zircons, likely derived from the Laramide porphyry copper province of southern Arizona and southwestern New Mexico. Paleoflow indicators suggest the third change in provenance was complete by 65 Ma as recorded by the deposition of the Paleocene Ojo Alamo Sandstone. However, our new U-Pb detrital-zircon results indicate this transition initiated ~8 m.y. earlier during deposition of the Campanian Kirtland Formation beginning ca. 73 Ma. This final change in provenance is interpreted to reflect the unroofing of surrounding Laramide basement blocks and a switch to local derivation. At this time, sediment entering the San Juan Basin was largely being generated from the nearby San Juan Mountains to the north-northwest, including uplift associated with early phases of Colorado mineral belt magmatism. Thus, the detrital-zircon spectra in the San Juan Basin document the transition from initial reworking of the Paleozoic and Mesozoic cratonal blanket to unroofing of distant basement-cored uplifts and Laramide plutonic rocks, then to more local Laramide uplifts.

†Deceased 21 July 2015, during preparation of manuscript

INTRODUCTION

U-Pb detrital-zircon (DZ) geochronology has played an integral role in deciphering sediment-dispersal patterns in Cretaceous and Paleogene strata of North America (e.g., Lawton and Bradford, 2011; Dickinson et al., 2012; Blum and Pecha, 2014; Bush et al., 2016; Sharman et al., 2017). DZ analyses allow for generation of a DZ fingerprint (Ross and Parrish, 1991) of the host rock, establishing provenance ties between host rock and source region(s) (Gehrels and Pecha, 2014), and for calculation of maximum depositional age of host rock (Surpless et al., 2006; Dickinson and Gehrels, 2009b), which can then be compared to biostratigraphic age where available. Combining DZ ages with fluvial paleocurrent information bolsters provenance ties and allows for regional paleogeographic reconstructions (Lawton and Bradford, 2011; Dickinson et al., 2012).

Cretaceous through Lower Eocene strata preserved in the San Juan Basin (SJB) in northwestern New Mexico and southwestern Colorado provide a unique opportunity to study spatial and temporal variations in sediment provenance using DZ geochronology. During the deposition of these sediments, the SJB region was flanked by the Sevier thrust belt, the Mogollon highlands rift shoulder, and was also influenced by Laramide tectonism (ca. 75–50 Ma). Understanding how these surrounding tectonic elements influenced sediment delivery to the Four Corners region, particularly the SJB, is the overall goal of this research.

Here we synthesize new and existing DZ data from Cretaceous and Paleogene strata and combine the observations with paleoflow information to make provenance assessments and paleogeographic interpretations. We also use the DZ ages to refine maximum depositional ages of the units by comparing them with biostratigraphic ages. Our new U-Pb DZ data indicate that three distinct changes in sediment provenance occur in the Cretaceous through Eocene section of the SJB. The results track changes in sediment routing from initial reworking of the Paleozoic and Mesozoic cratonal blanket to unroofing of distant basement-cored uplifts and Laramide plutonic rocks, then to more local Laramide uplifts. The results also provide additional clarity in sediment routing during the transition from Sevier retroarc thrusting through foreland basin partitioning during the Laramide, providing important insights into sediment-dispersal patterns and paleogeographic reconstructions. These new results fill in gaps from previous DZ studies (e.g., Dickinson and Gehrels, 2008; Gehrels et al., 2011; Lawton and Bradford, 2011; Dickinson et al., 2012) of Paleozoic and Mesozoic Colorado Plateau stratigraphy and Paleogene units (Dickinson et al., 2010; Donahue, 2016).

GEOLOGIC SETTING

The Four Corners region was part of an expansive late Mesozoic Cordilleran foreland basin system (Fig. 1) related to loading of the Sevier retroarc fold and thrust belt to the west (Armstrong, 1968; Jordan, 1981; DeCelles, 2004) and flanked on the southwest by the Mogollon highlands rift shoulder, a high-standing structural feature that formed at the same time as the Bisbee-McCoy basin (Dickinson and Lawton, 2001b; Lawton, 2004; Lucas, 2004; Dickinson and Gehrels, 2008). Immediately west of both of these features was the Cordilleran magmatic arc, which was assembled in response to continuous subduction of the Farallon plate along the western coast of North America from Permian (ca. 284 Ma) through early-middle Paleogene time (Dickinson, 2004).

Beginning in Late Campanian (ca. 75 Ma) time, deformation and magmatism translated inland in response to flat-slab subduction of the Farallon plate, creating the Laramide Province (Coney and Reynolds, 1977; Dickinson and Snyder, 1978; Bird, 1988; Miller et al., 1992; English et al., 2003; Saleeby, 2003; Liu et al., 2010). This change in plate dynamics partitioned the once-continuous Cordilleran foreland basin into a series of isolated intra-foreland basins and intervening basement-cored uplifts (Dickinson et al., 1988; Cather, 2004). In the Four Corners region, these uplifts are typically in the form of broad monoclines (e.g., Hogback monocline) or high-angle, fault-bounded basement blocks (e.g., Nacimiento uplift). Six distinct Laramide-age basins (San Juan, Raton, Galisteo–El Rito, Baca, Carthage–La Joya, and the Sierra Blanca) (Fig. 1) preserve varying thicknesses of Cretaceous–Eocene strata (Cather, 2004).

Late Cretaceous through Paleogene uplift and subsequent erosion have played a significant role in the formation of the current Colorado Plateau geomorphology (Elston and Young, 1991). Estimates of the thickness of pre-Cretaceous Mesozoic strata eroded from the Colorado Plateau range from ~3000 to 5000+ ft (~1000–1500 m), with thickness increasing from south-southeast to north-northwest (Wilson, 1967; Pederson et al., 2002; Lazear et al., 2013). It is also estimated that an additional ~1000–3000 ft (~300–1000 m) of Cretaceous strata were removed during Cenozoic beveling (Wilson, 1967; Epis and Chapin, 1975; Evanoff and Chapin, 1994; Pazzaglia and Kelley, 1998). This extensive erosion resulted in removal of most Cretaceous and younger rocks, leaving a wide region around Four Corners predominantly devoid of the entire Cretaceous section. The San Juan Basin (SJB) in northwestern New Mexico and southwestern Colorado is an exception, preserving a sequence of Cretaceous and younger sediments exceeding 6000 ft (~2000 m) in total thickness. The SJB represents the best preserved, deepest, and most comprehensive section that characterizes the Cretaceous/Paleogene stratigraphy of the region.

San Juan Basin

We define the SJB as the contiguous area that encompasses Lower Cretaceous through Eocene strata preserved in northwestern New Mexico and southwestern Colorado (Figs. 1 and 2). It is a structurally-bound intra-foreland basin that encompasses more than 46,000 km^2. It developed coevally with the adjacent Laramide tectonic features: San Juan (Needle Mountains) uplift to the north, Archuleta anticlinorium and/or San Juan sag to the northeast, Nacimiento uplift on the east, Zuni uplift to the south, Defiance uplift on the west, and Hogback monocline to the northwest (Kelley, 1950, 1951, 1957) (Fig. 2). Differential subsidence and sedimentation across the basin began in Campanian time, demonstrated by the deposition of the Lewis Shale (Ayers et al., 1994; Cather, 2003, 2004). Laramide accommodation within the interior basin is manifested in an asymmetrical synform with an arcuate axis that mimics the trend of bounding uplifts (Fig. 2) (Cather, 2003, 2004). Stratigraphic units in the SJB are relatively flat lying to shallow dipping, except along the eastern and northern margins of the basin. On the east side of the basin along the Nacimiento uplift, Lewis shale and younger sediments are highly attenuated and oriented vertically, showing growth strata relationships that indicate deposition was influenced by the developing Nacimiento thrust from ca. 80 to 50 Ma (Baltz, 1967; Molenaar, 1983). Steeply dipping units also occur along the northern margin of the basin where they have also been influenced by Laramide tectonism.

The Cretaceous and Eocene rocks preserved in the SJB are predominantly composed of interfingering marine and nonmarine sedimentary rocks (Fig. 3). The Cretaceous strata were deposited during basinwide cycles of transgression and regression of an expansive epicontinental sea (Fassett and Hinds, 1971); Tertiary strata were deposited in nonmarine, dominantly fluvial settings. Detailed geologic and sedimentologic descriptions and/or background of each unit can be found in Craigg (2001).

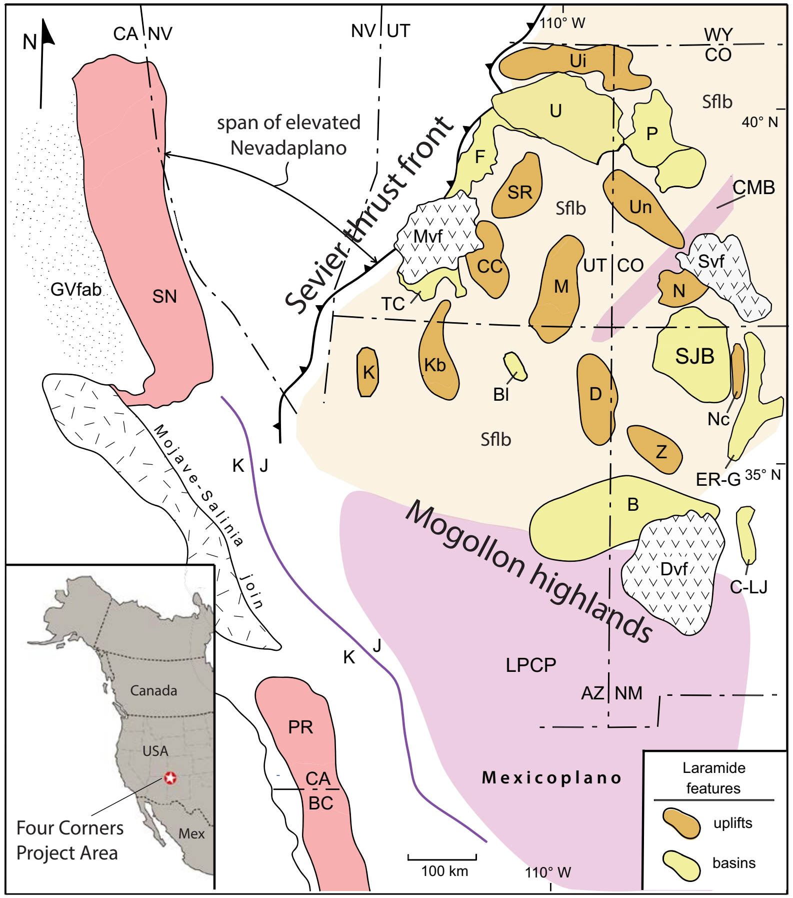

Figure 1. Tectonic elements map of southwestern North America including the location of the San Juan Basin (SJB) in relation to major Mesozoic and Cenozoic structural features of the North American Cordillera: PR—Peninsular Ranges; SN—Sierra Nevada; GVfab—Great Valley forearc basin; Sflb—Sevier foreland basin. Laramide basins (Maastrichtian–Paleogene) (Dickinson et al., 1988, 2012; Beard et al., 2010; Cather, 2004; Lawton, 2008): B—Baca; Bl—Black Mesa; C-LJ—Carthage–La Joya; ER-G—El Rito–Galisteo; F—Flagstaff; P—Piceance; SJB—San Juan; TC—Table Cliff; U—Uinta. Laramide uplifts (Kelley, 1955; Dickinson et al., 1988, 2012): CC—Circle Cliffs; D—Defiance; Kb—Kaibab; K—Kingman; M—Monument; N—Needle Mountains; Nc—Nacimiento; SR—San Rafael; Ui—Uinta; Un—Uncompahgre; Z—Zuni. Purple line denotes approximate boundary between dominantly Cretaceous (K) arc plutons (westward) and dominantly Jurassic (J) and older arc plutons (eastward) (Dickinson et al., 2012). Laramide-age magmatism: CMB—Colorado mineral belt; LPCP—Laramide porphyry copper province. Oligocene (post-Laramide) volcanic fields: Mvf—Marysvale; Dvf—Mogollon-Datil; Svf—San Juan. States: AZ—Arizona; BC—Baja California; CA—California; CO—Colorado; NV—Nevada; NM—New Mexico; UT—Utah; WY—Wyoming. Figure restored palinspastically after Dickinson (2011) and modified from Dickinson et al. (2012).

Four Corners Depositional Environments and Paleoflow Directions

Upper Jurassic–Lower Cretaceous Paleoflow (Upper Jurassic [163.5–145.0 Ma]; Timescale Based on Gradstein et al., 2012, Morrison Formation through Lower Cretaceous [145.0–100.5 Ma] Burro Canyon Formation)

Paleodrainage patterns on the Colorado Plateau document flow toward the northeast and east within the Upper Jurassic (Kimmeridgian–Tithonian) Morrison Formation (Craig et al., 1955; Peterson, 1984; Currie, 1997; Robinson and McCabe, 1998; Dickinson and Gehrels, 2008). Fluvial paleocurrent trends within the Lower Cretaceous Cedar Mountain and Burro Canyon Formations are generally easterly and northeasterly (Harris, 1980; Craig, 1981; Tschudy et al., 1984; Aubrey, 1992, 1996; Currie, 1998, 2002; Kirkland and Madsen, 2007; Dickinson and Gehrels, 2008), with a few restricted measurements having a northerly trend (Dickinson and Gehrels, 2008).

Sub-Dakota Unconformity

The southwestern margin of the Colorado Plateau, including portions of the future SJB, was stripped of several hundred meters of Triassic and Jurassic strata by NE-flowing rivers prior to early Late Cretaceous deposition of the Dakota Formation (Dickinson, 2013). This beveling of the NE margin of the pre-Laramide Mogollon highlands reflects Early Cretaceous uplift and erosion, which reworked older strata and redistributed older sediments.

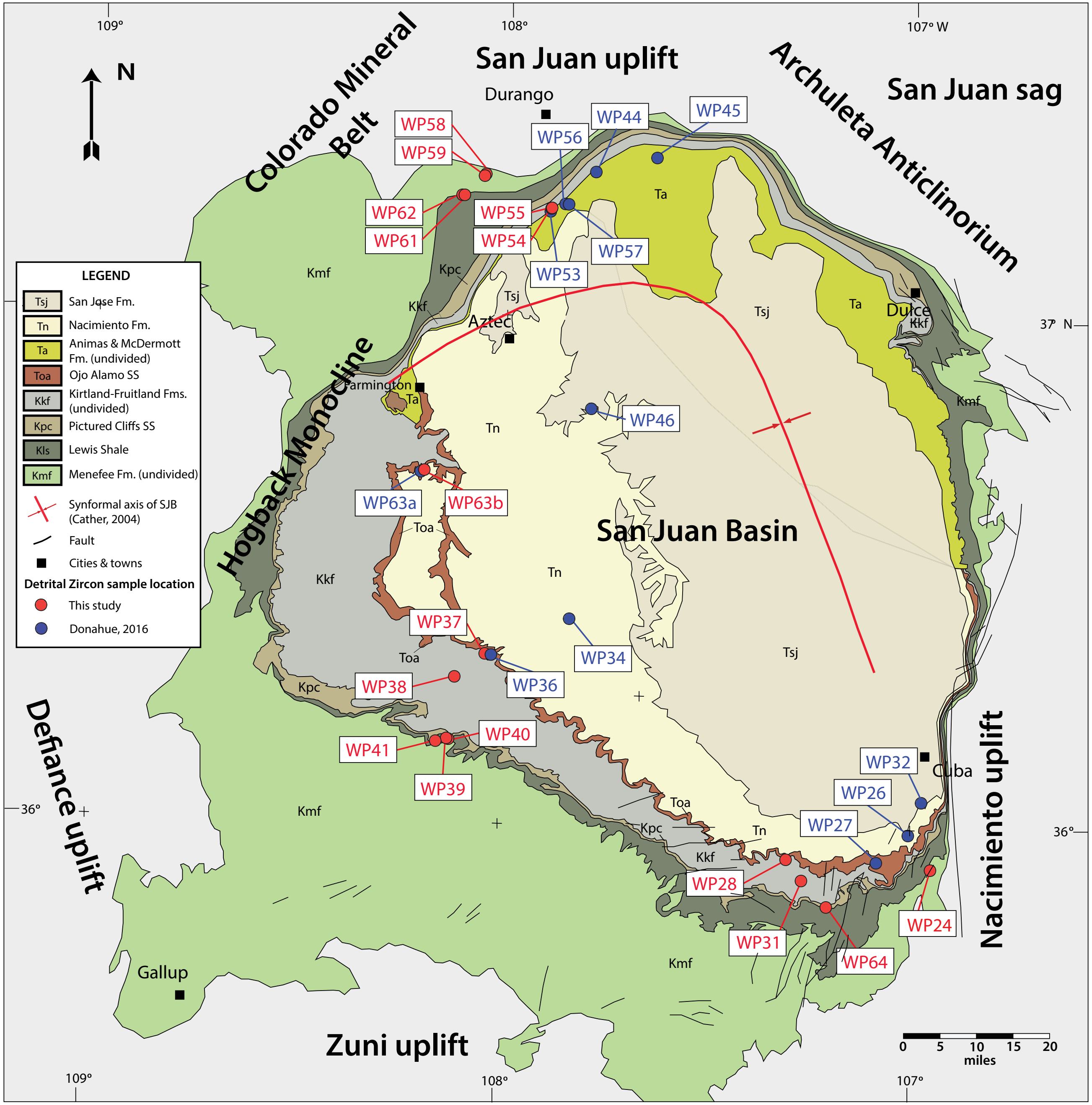

Figure 2. Simplified geologic map of the San Juan basin (SJB), northwestern New Mexico and southwestern Colorado. Surrounding Laramide features indicated in bold print: Colorado mineral belt, San Juan uplift, San Juan sag (Brister and Chapin, 1994), Archuleta anticlinorium, Nacimiento uplift, Zuni uplift, Defiance uplift, Hogback monocline. Detrital-zircon samples indicated with sample number (e.g., WP41) and color coded by reference: red (this study); blue (Donahue, 2016). Base geologic map modified from New Mexico Bureau of Geology and Mineral Resources (2003), Geologic map of New Mexico, 1:500,000.

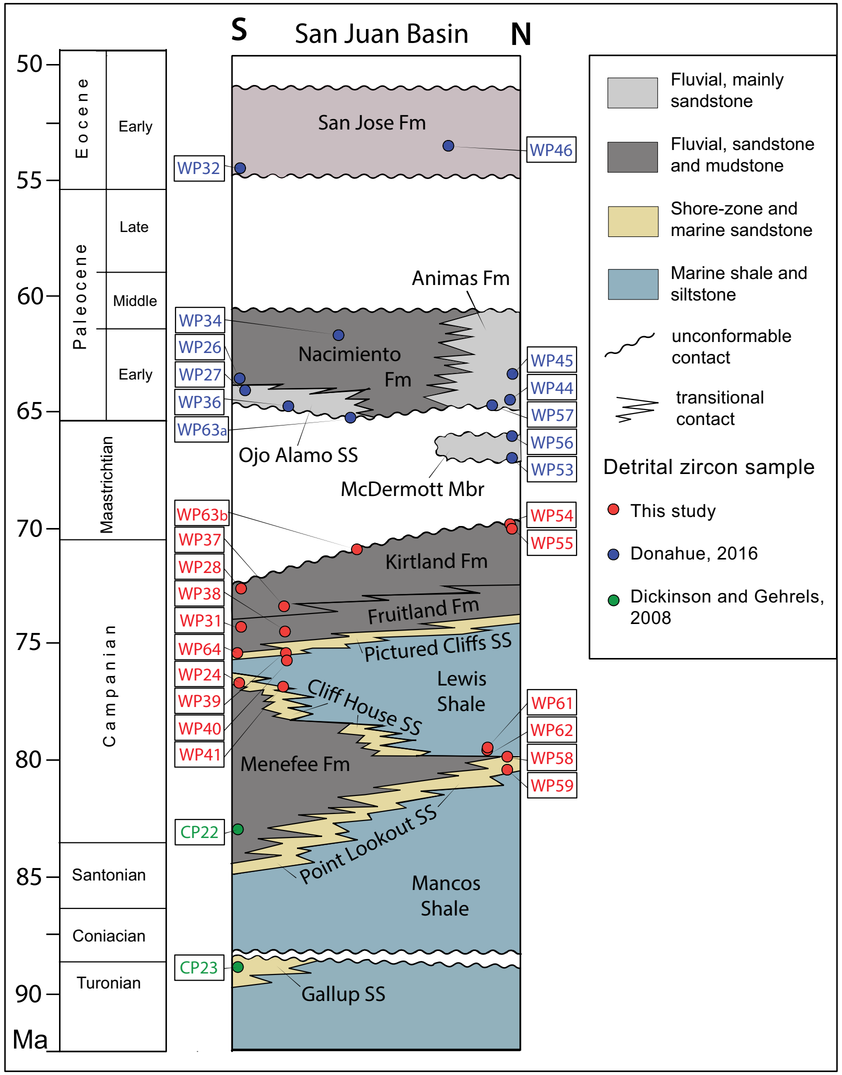

Figure 3. Schematic stratigraphic column of Cretaceous (Late Turonian) through Eocene strata of the San Juan basin, modified from Cather (2003, 2004). Detrital-zircon samples indicated with detrital-zircon sample number (e.g., WP24) and color-coded by reference: red (this study); blue (Donahue, 2016); green (Dickinson and Gehrels, 2008). Geologic Timescale based on Walker and Geissman (2009).

Upper Cretaceous Paleoflow (Coniacian [89.8–86.3 Ma] Mancos Shale through Campanian/Maastrichtian [83.6–66 Ma] Kirtland Formation)

The east-northeast paleoflow direction remained relatively constant through Late Cretaceous time (Fig. 4), as shown by deltaic systems on the margin of the Western Interior Seaway (Cather et al., 2012). The combination of paleocurrents and paleoshoreline migration (Cumella, 1983; Molenaar, 1983) during Mancos-Mesaverde sedimentation records sediment transport toward the interior of the Cordilleran foreland basin and the Great Plains region (Cumella, 1983; Dickinson and Gehrels, 2008). This sedimentation transport direction persisted through a series of regressive and transgressive cycles beginning with the Gallup Sandstone and continuing through the coastal facies (beach sand) deposits of Pictured Cliffs Sandstone, including the intervening Mancos Shale, Point Lookout Sandstone, and Menefee Formation.

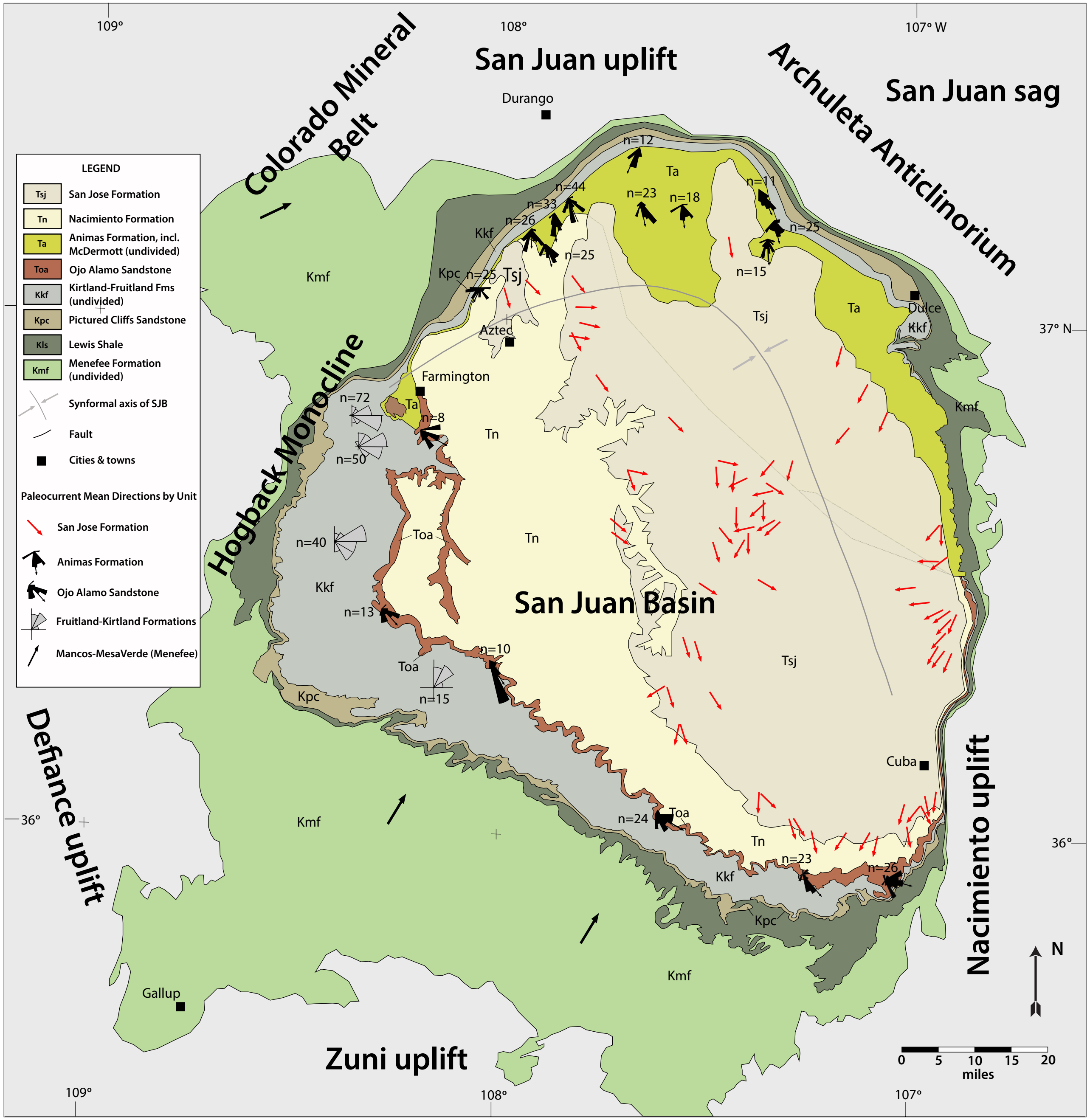

Figure 4. Paleocurrent map of Cretaceous through Eocene strata of the San Juan basin, northwestern New Mexico and southwestern Colorado. Paleocurrent trends are represented as azimuthal vectors with north to the top or shown in rose diagrams and overlain on simplified geologic map of the San Juan Basin (SJB). n = ## is the number of measurements included in each rose diagram. Statistics and values for the paleocurrent vector means for the San Jose Formation (red arrows) are in Smith (1988) and for the Menefee (black arrows) are in Cumella (1983). Paleoflow indicators are from the following sources: Kmf—Cumella (1983); Molenaar (1983); Dickinson and Gehrels (2008); Kpc—Hunt (1984); Hunt and Lucas (1992); Kkf—Dilworth (1960); Fassett and Hinds (1971); Cather (2004); Toa—Powell (1972); Lehman (1985); Klute (1986); Cather (2004); and Sikkink (1987); Ta—Sikkink (1987); Tsj—Smith (1988, 1992); Klute (1986). Base geologic map modified from New Mexico Bureau of Geology and Mineral Resources (2003), Geologic map of New Mexico 1:500,000.

The late Campanian Fruitland Formation (ca. 76–73 Ma), which represents a distal facies of the final regression of the Late Cretaceous seaway, locally intertongues with the Pictured Cliffs Sandstone where it formed in overbank deposits within backshore lowlands (Fassett, 2009). The landward facies depositional model for the Pictured Cliffs Sandstone consists of a deltaic complex in the northwestern basin and a barrier shoreline to the southeast (Erpenbeck, 1979; Flores and Erpenbeck, 1981). The paleoshoreline during Pictured Cliffs Sandstone deposition generally trended northwest-southeast, with inferred paleoflow to the northeast (Hunt, 1984; Hunt and Lucas, 1992).

The Late Campanian Kirtland Formation is composed of a southward-thinning package of fluvial sandstones and shales first described by Bauer (1916). It overlies the Fruitland Formation conformably and is overlain unconformably by the Ojo Alamo Sandstone. Fluvial paleocurrent directions in the south-central part of the SJB for the Fruitland-Kirtland interval indicate that streams depositing the Farmington Sandstone member flowed from southwest to northeast (Dilworth, 1960; Fassett and Hinds, 1971; Cather, 2004). However, in the western part of the basin, the paleocurrents generally trend easterly (Fig. 4) (Cather, 2004).

Upper Cretaceous through Paleocene Paleoflow—McDermott, Ojo Alamo, Animas, and Nacimiento

During the early Paleogene, paleoflow was toward the northeast in southern Utah and northern Arizona, with headwaters originating near the Sevier thrust belt and the Mogollon highlands (Young and McKee, 1978; Lawton, 1986; Elston and Young, 1991; Goldstrand, 1994). However, Paleocene paleoflow in the southern SJB beginning with the deposition of the Ojo Alamo Sandstone, shifted abruptly from northeast- to southeast-directed flow (Powell, 1972; Lehman, 1985; Klute, 1986; Cather, 2004), or southward-directed flow (Sikkink, 1987). The combination of these flow indicators and the presence of Laramide volcanic and/or plutonic, Paleozoic, and Precambrian detritus led some to interpret the Ojo Alamo Sandstone as recording the local initiation of Laramide uplift during late Maastrichtian–early Paleocene time (Fassett, 1985; Lehman, 1985). The presence of volcanic fragments and similar detrital constituents between the upper Kirtland Formation and Ojo Alamo Sandstone suggests they may have been derived from the same source (Klute, 1986).

The Paleocene McDermott Formation is only exposed in the northwestern margin of the SJB near Durango, Colorado (Figs. 2–4). Detailed studies of the McDermott Formation indicate that it contains multiple lithofacies and intraformational erosional surfaces (Lorraine and Gonzales, 2003; O'Shea, 2009). It contains a basal conglomerate and fines upward into interbedded sandstone and siltstone. The development of the McDermott Formation has been debated, from the traditional view as a volcaniclastic deposit (Reeside, 1924; McCormick, 1950; Barnes et al., 1954; Kottlowski, 1957; Sikkink, 1987), to a braided river deposit (O'Shea, 2009), to roof-flank detachment deposit that was remobilized and transported by debris flows and fluvial systems (Lorraine and Gonzales, 2003; Gonzales, 2010). Petrographic observations of igneous clasts present in the basal conglomerate (Gonzales, 2010; this study) suggest derivation from hypabyssal and plutonic intrusive rocks in the La Plata laccolitic complex. The vast majority of paleoflow indicators within the McDermott and Animas Formations document southerly flow toward the center of the SJB (Sikkink, 1987).

Lower Eocene Paleoflow (Ypresian [56.0–47.8 Ma] San Jose Formation)

The Lower Eocene San Jose Formation, initially described by Simpson (1948), has been the focus of subsequent studies of stratigraphy and paleogeography (Baltz, 1967; Smith et al., 1985; Smith, 1988, 1992). It is the youngest formation preserved within the SJB and unconformably overlies the Paleocene Nacimiento Formation in the south (with a gap of at least 5.6 m.y. in the vicinity of Mesa de Cuba; Fassett et al., 2010) and the Paleocene Animas Formation to the north. While it is likely the SJB originally contained Middle and Late Eocene strata, as adjacent Laramide basins do, only the Lower Eocene (Ypresian) remains after late Cenozoic erosion. The San Jose Formation preserves the final synorogenic sedimentation during waning Laramide activity.

Paleoflow within the San Jose Formation, as measured from large-scale trough cross-strata and pebble imbrications, is generally toward the south-southeast (Fig. 4) (Smith, 1988, 1992). Slight variations in the mean flow azimuth are indicated between various members of the formation, but the southeasterly direction is coincident with the underlying Paleocene stratigraphy (Klute, 1986; Sikkink, 1987), indicating similar paleoslope directions during the entire early Paleogene (Smith, 1988, 1992). Isolated conglomeratic sandstone lenses within the silt and mud–dominated sequence suggest sporadic sediment derivation directly from local basement-cored uplifts to the northwest.

Deposition of the San Jose Formation fluvial unit occurred in high-energy, low-sinuosity streams and associated muddy floodplains during late stages of the Laramide orogeny, as indicated by growth folds near the Nacimiento uplift (Baltz, 1967). Waning of the Laramide orogeny is recorded in the stratigraphic record by the Rocky Mountain erosion surface (RMES) (Evanoff and Chapin, 1994; Pazzaglia and Kelley, 1998) or Late Eocene erosion surface (Epis and Chapin, 1975).

METHODOLOGY

Sampling Strategy

Multiple samples were collected from each major stratigraphic unit within the SJB and contiguous areas (Fig. 3), and where outcrop and/or access allowed, samples were taken near the base and top of each unit in order to assess internal stratigraphic variability. Samples were also collected across the entire basin to evaluate spatial variations within individual units (Fig. 2). Previous DZ studies excluded some units (i.e., Lewis Shale) in order to avoid complications in the DZ signatures due to the effects of longshore sediment

2010 Four Corners samples -ExxonMobil COSA & Arizona Laserchron Center

Station number	UTM	UTM East	UTM North	Date	Location	TRIM sheet	U-Pb sample description
Cliff House SS-wp24	13S	321314	3973252	2010	San Juan Basin near Cuba, NM		fine grained arkosic ss, contains moderate amt of lithics and cemented w/ calcite (rxtn w/ HCl) or clay. Well sorted, local x-beds, tn to buff (yelowish brown). Sample taken from the LaVentana tongue-same outcrop as fig 1.2 (near mile 9.2 S of Cuba, NM (from NMGS, 1992 SJBIV Guidebook). Taken near base of thick, competent ss layer, above where it is interbedded w. the underlying Menefee, which consists of siltstones, shales, and clay or mudstones. Thickly bedded w/ local x-beds.
Lewis Shale-wp25	13S	321063	39977333	2010	San Juan Basin near Cuba, NM		Difficult to find outcrop…the Lewis is very friable and weathers easliy into a low-lying region w/ very little tomography and gently rolling hills. Sample taken in stream cut, taken from coarsest lenslens where there are also 1-2 cm cobbles. Matrix reacts to HCL
Nacimiento Fm-wp26	13S	318955	3983387	2010	San Juan Basin near Cuba, NM		Medium grained quartz arenite to arkose? SS. Interbedded w/ fine grained shales; forms "badlands" looking hills; predominantly qtz clasts w/ minor feldspars and lithics. Cemented w/ white clay…NO RXTN to HCL., probably deposited in a stream channel…beds not huge lateral extent.
Ojo Alamo SS-wp27	13S	311105	3978428	2010	San Juan Basin near Cuba, NM		Coarse grained arkosic SS w/ subangular grains; not well lithified, clast supported…little matrix; Qtz, feldspars, mica, lithics. Light brown in color (rusty in outcrop locally); forms overlapping sheet-like sequences.
Upper Kirtland-wp28	13S	297409	3976665	2010	San Juan Basin near Cuba, NM		Sample taken ~3' below the Kirtland-OjoAlamo contact. Taken from saniest layer in Kirtland (in vicinity); Sample consists entirely of the tan SS layer, but there are also purplish shale beds which are interbedded here (not sampled); Very fine to fine grained arkosic SS...qtz, feldspar w/ minor black lithics; DOES NOT RXCT w/ HCL.
Pictured Cliffs SS-wp29	13S	299447	3974650	2010	San Juan Basin, NM		Weathers like fruitland but it is a fine to med gr SS. Sample taken from coarsest lens within the unit; cemented w/ calcite (rxcts w/ acid); fine grained arkosic SS consisting of qtz,feldspar and minor lithics; sample contains abundant fossil twigs and some appear "coalish". SAME AS wp30
Pictured Cliffs SS-wp30	13S	299454	3974655	2010	San Juan Basin, NM		Weathers like fruitland but it is a fine to med gr SS. Sample taken from coarsest lens within the unit; cemented w/ calcite (rxcts w/ acid); fine grained arkosic SS consisting of qtz,feldspar and minor lithics; sample contains abundant fossil twigs and some appear "coalish". SAME AS wp 29

[1]Supplemental Item 1. Detrital-zircon sample descriptions, including GPS coordinates of sample localities. Please visit **http://doi.org/10.1130/GES01485.S1** or the full-text article on www.gsapubs.org to view Supplemental Item 1.

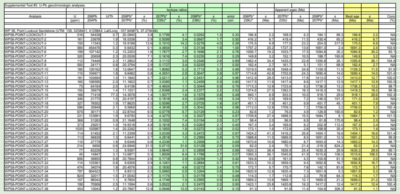

[2]Supplemental Item 2. Complete U-Pb analytical methods including exact laser used on each sample. Please visit **http://doi.org/10.1130/GES01485.S2** or the full-text article on www.gsapubs.org to view Supplemental Item 2.

transport (e.g., Dickinson and Gehrels, 2008). However, this study incorporated those samples for completeness and for statistical comparisons with the fluvial sediments.

DZ sample descriptions, including GPS coordinates of sample localities, can be accessed in Supplemental Item 1[1].

U-Pb Analytical Methods

Zircon grains were extracted from whole-rock samples using traditional methods of jaw crushing and pulverizing, followed by density separation using a Wilfley table and heavy liquids (methylene iodide). The resulting heavy-mineral fraction then underwent separation using a Frantz LB-1 magnetic barrier separator to isolate the zircons. A representative split of the entire zircon yield of each sample was incorporated into a 1-inch epoxy mount along with multiple fragments of the primary Sri Lanka (SL) zircon standard. The mounts were sanded down ~20 microns, polished using a 9-micron polishing pad, and backscattered electron (BSE) imaged using a Hitachi S-3400N scanning electron microscope (SEM). Prior to isotopic analysis, the mounts were cleaned in an ultrasound bath of 1% HNO_3 and 1% HCl in order to remove any residual common Pb from the surface of the mount.

U-Pb geochronology of single zircon crystals was conducted by laser ablation–multicollector–inductively coupled mass spectrometry (LA-MC-ICPMS) at the Arizona LaserChron Center (Gehrels et al., 2006, 2008). The isotopic analyses involved ablation of zircon using either a New Wave UP193HE excimer laser (analyses completed prior to May 2011) or a Photon Machines Analyte G2 excimer laser (analyses completed post–April 2011) coupled to a Nu Instruments HR-MC-ICPMS (see Supplemental Item 2[2] for complete U-Pb analytical methods including exact laser used on each sample).

Approximately 105 laser analyses were completed on each sample with only one U-Pb measurement per grain. Random grain selection was conducted using BSE images with rejection only of zircons that were too small to fit the entire 30-micron spot within its borders or those that contained cracks and/or inclusions that prohibited a clear spot placement.

U-Pb analytical data are presented here in age-distribution diagrams, which account for both analytical uncertainty and age of each analysis. These plots were generated by assuming normal distributions of age for each grain age, followed by the summing of all normal distributions into composites, which were then normalized to produce equal areas under the curves.

DETRITAL-ZIRCON U-Pb RESULTS

We report a total of 1520 new U-Pb laser analyses from 16 DZ samples of Cretaceous strata from the SJB in northwestern New Mexico and southwestern Colorado. Table 1 summarizes the DZ samples from this study, in addition to previously reported DZ samples used in reference comparisons. The complete U-Pb analytical results are reported in the Supplemental Item 2 (see footnote 2) and summarized below according to stratigraphic unit from oldest to youngest. Multiple samples were collected from each major unit, and the results are presented in composite age distributions (Fig. 5, composites a–f).

The maximum depositional age for each newly reported sample is presented in Table 1 (all maximum depositional ages are reported as weighted averages at 2 sigma). Samples were evaluated for maximum depositional age using "Tuffzirc" and "Unmix" age routines available in the Excel plug-in, Isoplot 3.60 (Ludwig, 2008), as well as calculating weighted averages. The calculated maximum depositional age results and associated plots can be found in Supplemental Item 2 (see footnote 2). In all cases the "Tuffzirc" and "Unmix" age routines yielded similar results as their counterpart weighted averages; therefore, the weighted averages are deemed as the robust maximum depositional age for each sample since they account for all internal and external errors.

Detrital-Zircon Results of Cretaceous Strata of the San Juan Basin

Point Lookout Sandstone

Two detrital-zircon samples (WP58 and WP59) of Point Lookout Sandstone yielded 195 reliable U-Pb analyses. Both samples produced a mix of Precambrian, Paleozoic, and Mesozoic ages, with similar age distributions. The composite age spectra (Fig. 5A) are dominated by Paleoproterozoic (39%) and Mesoproterozoic (25%) ages ranging from ca. 2100 to 1015 Ma (prominent age peaks at 1728, 1690, 1417, and 1113 Ma), isolated Neoproterozoic (2%) ages ranging from ca. 918 to 602 Ma, Paleozoic (7%) ages ranging from ca. 460 to 334 Ma (peaks at 421 and 349 Ma), and Mesozoic (27%) ages ranging from ca. 236 to 77 Ma (peaks at 167 and 85 Ma). U-Pb DZ maximum depositional ages for WP59 and WP58 are 85.1 ± 2.2 Ma and 84.6 ± 1.5 Ma, respectively.

Cliff House Sandstone

Two samples of Cliff House Sandstone (WP24 and WP41) yielded 195 robust U-Pb ages. The two samples yielded similar age ranges, but sample WP24 contained a significantly higher proportion of Mesozoic ages compared to WP41. The composite age distribution (Fig. 5B) is characterized by sparse Archean (5%) ages ranging from ca. 3350 to 2600 Ma (peak of 2723 Ma) and is dominated by Paleoproterozoic (24%) and Mesoproterozoic (35%) ages ranging from ca. 1920 to 1000 Ma (dominant age peaks of 1832, 1713, 1428, and 1062 Ma), isolated Neoproterozoic (3%) ages ranging from ca. 999 to 710 Ma, Paleozoic (10%) ages ranging from ca. 515 to 255 Ma (peak of 427 Ma), and Mesozoic (23%) ages ranging from ca. 235 to 76 Ma (dominant age peaks of 210, 173, 93, and 77 Ma). U-Pb DZ maximum depositional ages for WP41 and WP24 are 93.3 ± 2.8 Ma and 77.5 ± 1.9 Ma, respectively.

TABLE 1. U-Pb DETRITAL-ZIRCON SAMPLES OF CRETACEOUS AND PALEOGENE STRATA FROM THE SAN JUAN BASIN AND SURROUNDING REGION, INCLUDING REFERENCE SUBSETS FROM THE CORDILLERAN FORELAND (UTAH) AND NORTHERN FLANK OF THE MOGOLLON HIGHLANDS (ARIZONA)

Sample ID	Stratal unit	Stratal age (biostrat. age)	Location	U-Pb MDA	U-Pb reference
[4]NARCHU	Chuska	Eocene–Oligocene	Chuska Mountains		Dickinson et al., 2010
[4]COL12	Music Mountain	Paleogene	Peach Springs Wash		Dickinson et al., 2012
[4]COL13	Music Mountain	Paleogene	Duff Brown tank		Dickinson et al., 2012
WP32	San Jose Fm.	Early Eocene (55–50 Ma)	SJB	80.0 ± 2.6 Ma; 1.3 MSWD	Donahue, 2016
WP46	San Jose Fm.	Early Eocene (55–50 Ma)	SJB	71.9 ± 3.1 Ma; 0.41 MSWD	Donahue, 2016
WP26	Nacimiento Fm.	Paleocene (65–61 Ma)	SJB	72.0 ± 1.5 Ma; 1.2 MSWD	Donahue, 2016
WP34	Nacimiento Fm.	Paleocene (65–61 Ma)	SJB	69.9 ± 3.3 Ma; 3.4 MSWD	Donahue, 2016
WP44	Animas Fm.	Paleocene (66–60 Ma)	SJB	63.58 ± 1.22 Ma; 0.4 MSWD	Donahue, 2016
WP45	Animas Fm.	Paleocene (66–60 Ma)	SJB	70.4 ± 1.5 Ma; 1.6 MSWD	Donahue, 2016
WP57	Animas Fm.	Paleocene (66–60 Ma)	SJB	68.9 ± 1.2 Ma; 0.74 MSWD	Donahue, 2016
WP27	Ojo Alamo SS	Early Paleocene (66–65 Ma)	SJB	73.2 ± 2.9 Ma; 0.16 MSWD	Donahue, 2016
WP36	Ojo Alamo SS	Early Paleocene (66–65 Ma)	SJB	69.9 ± 2.4 Ma; 1.12 MSWD	Donahue, 2016
WP63a	Ojo Alamo SS	Early Paleocene (66–65 Ma)	SJB	Only one Maastrichtian age	Donahue, 2016
WP53	McDermott Mbr.	Maastrichtian (68–67 Ma)	SJB, nr. Durango	69.84 ± 1.10 Ma; 1.0 MSWD	Donahue, 2016
WP56	McDermott Mbr.	Maastrichtian (68–67 Ma)	SJB, nr. Durango	68.04 ± 0.75 Ma; 0.4 MSWD	Donahue, 2016
WP28	Kirtland Fm.	Late Camp.–Maast. (74–71.5 Ma)	SJB	70.6 ± 1.5 Ma; 1.09 MSWD	This paper
WP37	Kirtland Fm.	Late Camp.–Maast. (74–71.5 Ma)	SJB	75.8 ± 1.7 Ma; 1.7 MSWD	This paper
WP54	Kirtland Fm.	Late Camp.–Maast. (74–71.5 Ma)	SJB	74.4 ± 2.8 Ma; 0.12 MSWD	This paper
WP55	Kirtland Fm.	Late Camp.–Maast. (74–71.5 Ma)	SJB	75.1 ± 2.4 Ma; 0.49 MSWD	This paper
WP63b	Kirtland Fm.	Late Camp.–Maast. (74–71.5 Ma)	SJB	71.8 ± 1.7 Ma; 0.18 MSWD	This paper
WP31	Fruitland Fm.	Late Campanian (75.5–73.5 Ma)	SJB	73.7 ± 1.6 Ma; 0.41 MSWD	This paper
WP38	Fruitland Fm.	Late Campanian (75.5–73.5 Ma)	SJB	72.5 ± 1.4 Ma; 0.73 MSWD	This paper
WP39	Pictured Cliffs SS	Late Campanian (76.5–73.5 Ma)	SJB	76.9 ± 1.4 Ma; 0.89 MSWD	This paper
WP64	Pictured Cliffs SS	Late Campanian (76.5–73.5 Ma)	SJB	75.8 ± 1.4 Ma; 0.73 MSWD	This paper
WP40	Lewis Shale	Campanian (80.5–74.5 Ma)	SJB	75.6 ± 1.5 Ma; 1.2 MSWD	This paper
WP61	Lewis Shale	Campanian (80.5–74.5 Ma)	SJB	No Mesozoic ages present	This paper
WP62	Lewis Shale	Campanian (80.5–74.5 Ma)	SJB	No Mesozoic ages present	This paper
[1]P6GC	Grand Castle	Campanian	Parowan Canyon		Johnson et al., 2011
[1]WF6GC	Grand Castle	Campanian	Webster Flat		Johnson et al., 2011
[1]WP9GC	Grand Castle	Campanian	Paunsagunt Plateau		Johnson et al., 2011
[1]CP40	Capping Wahweap	Middle Campanian	Henrieville Creek		Dickinson and Gehrels, 2008
WP41	Cliff House SS	Middle Camp. (80.5–79.5 Ma)	SJB	93.3 ± 2.8 Ma; 0.14 MSWD	This paper
WP24	Cliff House SS	Middle Camp. (80.5–79.5 Ma)	SJB	77.5 ± 1.9 Ma; 0.87 MSWD	This paper
[3]KK1	Lower Kaiparowits	middle Campanian	Kaiparowits Plateau		Lawton and Bradford, 2011
CP22	Menefee Fm.	Early-middle Camp (85–78.5 Ma)	SJB		Dickinson and Gehrels, 2008
[1]2JL5	*Capping Wahweap*	*Early Campanian*	*Henrieville Creek*		*Larsen et al., 2010*
WP58	Point Lookout SS	Sant.–early Camp (85–80.5 Ma)	SJB	84.6 ± 1.5 Ma; 1.2 MSWD	This paper
WP59	Point Lookout SS	Sant.–early Camp (85–80.5 Ma)	SJB	85.1 ± 2.2 Ma; 1.1 MSWD	This paper
CP23	Gallup SS	Turonian (91–88.5 Ma)	SJB		Dickinson and Gehrels, 2008
[3]CP39	Upper Wahweap	Early Campanian	Henrieville Creek		Dickinson and Gehrels, 2008
[3]1JL5	*Lower Wahweap*	*Early Campanian*	*Star Seep*		*Larsen et al., 2010*
[3]CP33	Ferron	Turonian	Dry Wash		Dickinson and Gehrels, 2008
[3]COL11	Ferron	Turonian (91–88.5 Ma)	Caineville Gap		Dickinson et al., 2012
CP27	Burro Canyon Fm.	Aptian–Albian	SJB		Dickinson and Gehrels, 2008
CP53	Burro Canyon Fm.	Aptian–Albian	SJB		Dickinson and Gehrels, 2008
[4]CP9	Toreva	Turonian	Black Mesa		Dickinson and Gehrels, 2008
[2]5-6B	Buckhorn	Aptian	Buckhorn Draw		Larsen et al., 2010
[2]CP32	Buckhorn	Aptian	San Rafael River		Dickinson and Gehrels, 2008
[2]RRR12	Poison Strip	Aptian	Ruby Ranch		Ludvigson et al., 2010

Notes: All U-Pb ages were determined by laser ablation–inductively coupled plasma mass spectrometry (LA-ICPMS) at the Arizona LaserChron Center, University of Arizona, except samples in italics, which were determined by thermal ionization mass spectrometry (TIMS) at the Australian National University. Reference detrital-zircon (DZ) subsets from Dickinson et al. (2012); subsets are indicated using number designation in sample ID column as follows: [1]Southern Sevier reference subset J; [2]Northern Sevier reference subset I; [3]Sevier and Mogollon reference subset K; [4]Mogollon reference subset M. Biostratigraphic (biostrat.) ages from ammonite zones (figure 6 from Nummedal, 2004; figure 2 and table 1 from Cather, 2004) as calibrated by Gradstein et al. (2012) (Walker and Geissman [2009]). Maximum depositional ages (MDA) are reported for newly reported samples that contain U-Pb ages within 10% of reported biostratigraphic age. Abbreviations: Camp.—Campanian; Fm.—Formation; Maas.—Maastrichtian; Mbr.—Member; MSWD—mean square of weighted deviates; nr.—near; Sant.—Santonian; SJB—San Juan Basin; SS—sandstone.

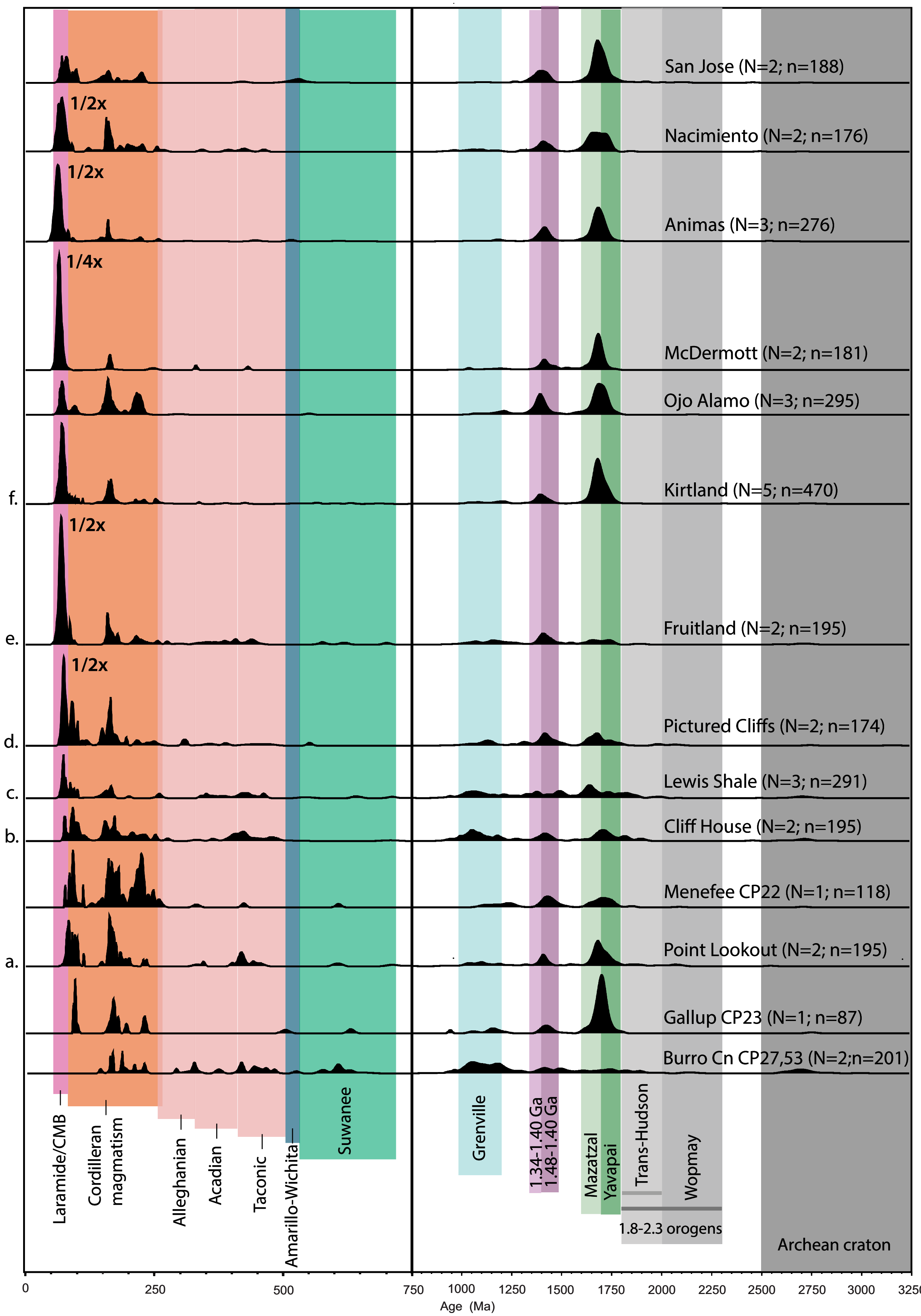

Figure 5. Normalized age distribution curves of composite detrital-zircon (DZ) samples (0–3250 Ma) stacked from oldest (Burro Canyon Formation) to youngest (San Jose Formation). N is the number of samples composited, and n is the total number of DZ ages in each composited distribution. Colored bands (A–M) correspond to the North American crustal province map (Fig. 6). 0–750 Ma scale is expanded to show the young end of the age spectra in greater detail. The bold "1/2x" and "1/4x" mean the tallest peaks from those particular age spectra have been reduced by 50% and 75% in height, respectively. This was done to enhance the other age peaks that would be diminished otherwise. CMB—Colorado mineral belt; Cn—Canyon.

Lewis Shale

Three samples of Lewis Shale (WP40, WP61, and WP62) yield a complex age distribution (Fig. 5C) consisting of scattered Archean (5%) ages ranging from ca. 3210 to 2504 Ma (peak at 2742), and Paleoproterozoic (32%) and Mesoproterozoic (38%) zircons ranging in age from ca. 2095 to 1015 Ma (prominent age peaks at 1736, 1642, 1491, 1388, and 1076 Ma), scattered Neoproterozoic (5%) grains ranging from ca. 995 to 552 Ma, Paleozoic (8%) grains ranging from ca. 540 to 260 Ma (peak at 434 Ma). There is a significant fraction of Mesozoic (12%) ages that range from ca. 202 to 72 Ma (pronounced age peaks at 168 and 75 Ma). U-Pb DZ maximum depositional age for WP40 is 75.6 ± 1.5 Ma. Lewis Shale samples WP61 and WP62 did not contain any Mesozoic zircons; so maximum depositional ages were not calculated for these samples.

Pictured Cliffs Sandstone

Two samples of Pictured Cliffs Sandstone (WP39 and WP64) yielded 174 robust U-Pb zircon ages. The combined distribution (Fig. 5D) contains a few scattered Archean (2%) ages ranging from ca. 3647 to 2760 Ma and Paleozoic (5%) ages ranging from ca. 554 to 255 Ma but is dominated by Paleoproterozoic (22%) and Mesoproterozoic (28%) ages ranging from ca. 2108 to 1039 Ma (prominent age peaks of 1692, 1418, 1338, and 1154 Ma) and Mesozoic (41%) ages ranging from ca. 250 to 72 Ma (distinct age peaks at 166, 94, and 76 Ma), plus isolated Neoproterozoic (2%) ages ranging from ca. 958 to 553 Ma. U-Pb DZ maximum depositional ages for WP39 and WP64 are 76.9 ± 1.4 Ma and 75.8 ± 1.4 Ma, respectively.

Fruitland Formation

Two samples of Fruitland Formation (WP31 and WP38) produced 195 robust U-Pb ages. The composite age distribution (Fig. 5E) shows a few scattered Archean (2%) ages, Paleoproterozoic (11%) and Mesoproterozoic (28%) ages ranging from ca. 1920 to 1009 Ma (age peaks of 1762, 1685, 1421, 1183, and 1094 Ma), isolated Neoproterozoic (2%) ages ranging from ca. 703 to 579 Ma, and scattered Paleozoic (8%) ages ranging from ca. 444 to 59 Ma. The spectrum is dominated by Mesozoic (49%) ages ranging from ca. 245 to 66 Ma (subordinate age peaks at 219 and 161 Ma and a dominant depositional age peak at 74 Ma). U-Pb DZ maximum depositional ages for WP31 and WP38 are 73.7 ± 1.6 Ma and 72.5 ± 1.4 Ma, respectively.

Kirtland Formation

A total of 470 U-Pb laser analyses have been completed on five samples of Kirtland Formation (WP28, WP37, WP54, WP55, and WP63b), and the composite age distribution (Fig. 5F) reveals a relatively simple distribution with six main age peaks. The Kirtland Formation contains isolated Archean (1%) ages ranging from ca. 2770 to 2560 Ma but is dominated by Paleoproterozoic (55%) and Mesoproterozoic (17%) ages ranging from ca. 1895 to 1040 Ma (prominent peaks at 1689, 1409, 1230, and 1109 Ma) and Mesozoic (24%) ages ranging from ca. 230 to 67 Ma (main peaks at 168 and 72 Ma), isolated Neoproterozoic (1%) ages ranging from ca. 954 to 569 Ma, scattered Paleozoic (2%) ages ranging from ca. 534 to 254 Ma, and a few Cenozoic (<1%) ages between 65 and 63 Ma. U-Pb DZ maximum depositional ages for WP37, WP55, WP54, WP63b, and WP28 are 75.8 ± 1.7 Ma, 75.1 ± 2.4 Ma, 74.4 ± 2.8 Ma, 71.8 ± 1.7 Ma, and 70.6 ± 1.5 Ma, respectively.

INTERPRETATION OF DETRITAL-ZIRCON AGES

U-Pb detrital-zircon age signatures of the Cretaceous through Eocene strata of the SJB contain distinct age distributions that can be linked to particular source regions (Fig. 5). The presence or absence of specific age peaks allows for first-order provenance assessment with respect to the basement geology of the North America, which is well known and can be summarized by its principal source components (Fig. 6). Given that these are Cretaceous and younger strata, and the likelihood of recycling older zircon through younger strata before deposition in the SJB is high, therefore, comparisons were made with reference DZ age subsets from Dickinson et al. (2012), which allowed us to identify source regions for the detrital zircons preserved in the SJB. These reference subsets contain detritus shed from reworking of the sedimentary cover that capped the adjacent Sevier and Mogollon highlands and distributed them peripherally during Cretaceous and Paleogene time.

The North American crustal province map (Fig. 6) was originally based on Hoffman (1988) and later adapted from Gehrels et al. (2011) and Laskowski et al. (2013) and is color-coded to match age bands of potential source regions on DZ U-Pb age-probability diagrams (Figs. 5 and 7–11). Kolmogorov-Smirnov (K-S) statistical test results comparing the detrital-zircon results can be found in Supplemental Item 3[3]. The ubiquitous Proterozoic ages in our data, which correlate with the Yavapai (ca. 1.8–1.7 Ga)-Mazatzal (ca. 1.7–1.6 Ga) provinces and the ca. 1.48–1.34 magmatic province, reflect local basement geology of the greater Four Corners region.

To assess the provenance of the Cretaceous through Eocene section preserved in the SJB, we include previously reported DZ results from within the basin (Table 1). Ojo Alamo Sandstone, Animas Formation–McDermott Member, Animas Formation, Nacimiento Formation, and San Jose Formation are from Donahue (2016). Burro Canyon Formation, Mancos shale, and Menefee Formation DZ results are from Dickinson et al. (2012). DZ data from the Dakota Sandstone (Ludvigson et al., 2010; Dickinson et al., 2012) were initially evaluated (probability density plot comparisons are available in the Dakota tab located in Supplemental Item 2 [footnote 2]) in the same manner as the SJB DZ samples. However, the only available DZ data from the Dakota Sandstone were collected far outside the SJB and therefore are not included in this summary.

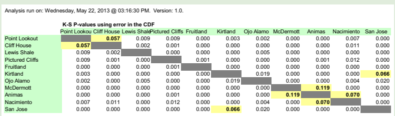

Analysis run on: Wednesday, May 22, 2013 @ 03:16:30 PM. Version: 1.0.

K-S P-values using error in the CDF

	Point Lookou	Cliff House	Lewis Shale	Pictured Cliffs	Fruitland	Kirtland	Ojo Alamo	McDermott	Animas	Nacimiento	San Jose
Point Lookout		**0.057**	0.009	0.009	0.000	0.003	0.002	0.000	0.000	0.007	0.000
Cliff House	**0.057**		0.002	0.001	0.000	0.000	0.000	0.000	0.000	0.011	0.000
Lewis Shale	0.009	0.002		0.000	0.000	0.000	0.005	0.000	0.000	0.000	0.000
Pictured Cliffs	0.009	0.001	0.000		0.001	0.000	0.000	0.000	0.001	0.012	0.000
Fruitland	0.000	0.000	0.000	0.001		0.000	0.000	0.000	0.000	0.000	0.000
Kirtland	0.003	0.000	0.000	0.000	0.000		0.019	0.000	0.000	0.000	**0.066**
Ojo Alamo	0.002	0.000	0.005	0.000	0.000	0.019		0.000	0.000	0.004	0.020
McDermott	0.000	0.000	0.000	0.000	0.000	0.000	0.000		**0.119**	0.000	0.000
Animas	0.000	0.000	0.000	0.001	0.000	0.000	0.000	**0.119**		**0.070**	0.000
Nacimiento	0.007	0.011	0.000	0.012	0.000	0.000	0.004	0.000	**0.070**		0.000
San Jose	0.000	0.000	0.000	0.000	0.000	**0.066**	0.020	0.000	0.000	0.000	

[3]Supplemental Item 3. Kolmogorov-Smirnov (K-S) statistical test results for comparison of detrital-zircon results. Please visit http://doi.org/10.1130/GES01485.S3 or the full-text article on www.gsapubs.org to view Supplemental Item 3.

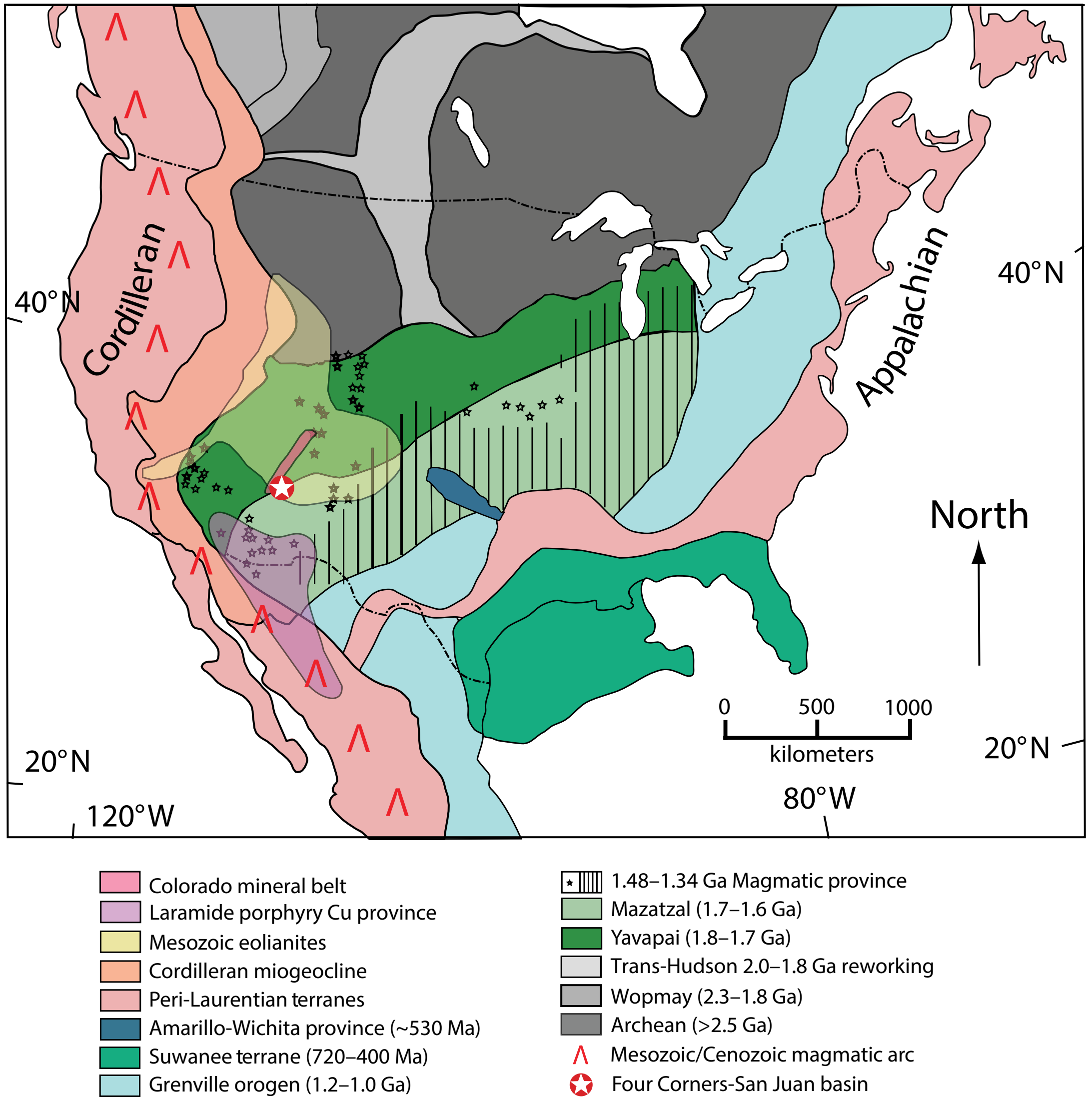

Figure 6. North American crustal province map. Age domains are color coded to match the age-probability diagrams in Figures 4 and 6–9. Adapted from Laskowski et al. (2013) and Gehrels et al. (2011), which were originally based on Hoffman (1988). Distribution of Mesozoic eolianites from Leier and Gehrels (2011).

Ages of Possible Source Regions

We first explore the young (<285 Ma) grains within each age spectrum to elucidate significant differences and similarities between various SJB strata. Detrital zircons <285 Ma in age from Upper Cretaceous through Eocene strata of the SJB could have been derived from any of the following sources.

1. Permian–Triassic grains (ca. 284–202 Ma) are potentially derived from the Permo-Triassic east Mexico arc (ca. 284–232 Ma) and its cryptic extensions westward across Sonora (Torres et al., 1999; Dickinson and Lawton, 2001a; Arvizu et al., 2009) into the Mojave region or from the nascent Cordilleran arc (<245 Ma) extending across northern Mexico and up the length of California (Busby-Spera, 1988; Barth and Wooden, 2006).

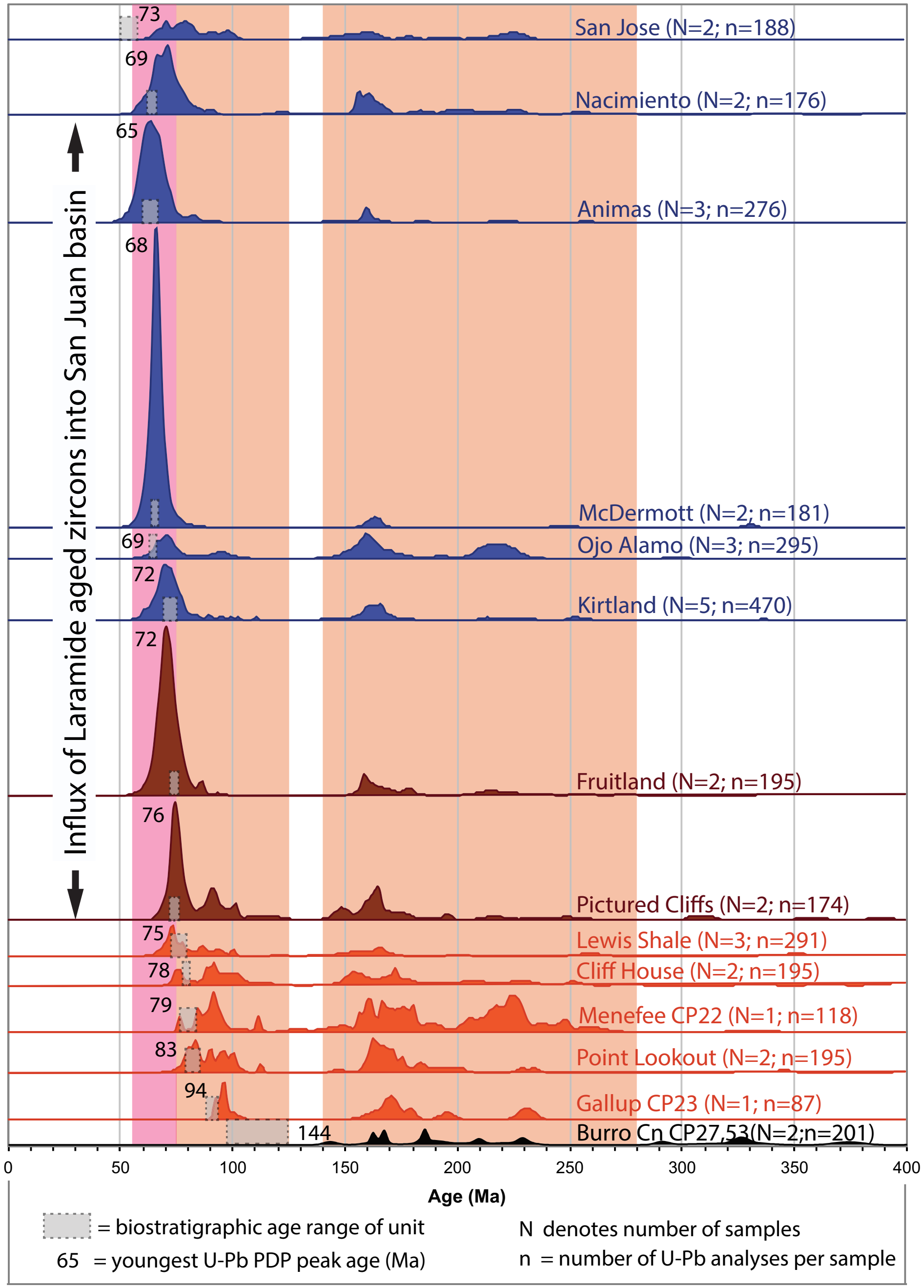

Figure 7. Normalized age distribution curves of composite detrital-zircon (DZ) samples (0–400 Ma only). Profound influx of near-depositional-age grains indicating sediment input from either the Laramide porphyry copper province in southern Arizona and/or New Mexico or northern Sonora, Mexico and/or input from the Colorado mineral belt. Age spectra are color coded by the four groupings indicated in Figure 6. N is the number of samples composited, and n is the total number of DZ ages in each composited distribution. Colored bands (A–M) correspond to Tables 1 and 2 indicating the various Cordilleran magmatic episodes. Cn—Canyon; PDP—probability density plot.

2. Triassic grains (ca. 245–201 Ma) are potentially derived from the Nazas arc of northern Mexico and its extensions westward through Arizona and up the length of eastern California (Lawton and McMillan, 1999; Haxel et al., 2008).
3. Late Jurassic grains (ca. 160–150 Ma) are potentially sourced from a major pulse of granitic magmatism in the Sierra Nevada (Ducea, 2001).
4. Cretaceous grains (ca. 125–80 Ma) are potentially sourced from the evolving Cordilleran arc of California, Baja California, and coastal Sonora following the Early Cretaceous accretion of Guerrero. A second major pulse of granitoid magmatism took place in the Sierra Nevada arc ca. 98–86 Ma (Ducea, 2001).
5. Latest Cretaceous grains (ca. 80–65 Ma) are potentially sourced from the Laramide magmatic arc that migrated inland to Mexico-Arizona-Nevada in response to shallow Farallon plate subduction or from laccoliths and/or plutons at the southwestern end of the Colorado mineral belt, which formed in response to the same migratory phase of Cordilleran magmatism.
6. Paleogene ca. 65–60 Ma grains are potentially sourced from continued Laramide and Colorado mineral belt magmatism. See Figure 6 for approximate locations of the similar-aged eastward-migrating southern Arizona and Colorado mineral belt magmatism.
7. Recycling of Permian–Triassic grains from the Chinle Formation (Upper Triassic) and of Permian–Triassic and Jurassic grains from either the Morrison Formation (Upper Jurassic) or Burro Canyon Formation (Lower Cretaceous) is possible, although only proximal reaches of those depositional systems on the northern flank of the Jurassic–Cretaceous Mogollon highlands rift shoulder of the Bisbee basin could have been eroded before onlap by the early Late Cretaceous Dakota Formation protected them from erosion until Laramide deformation in latest Cretaceous and Paleogene time.

Due to the broad lull in Cordilleran arc magmatism during the Early Cretaceous (ca. 140–125 Ma; Armstrong and Ward, 1993; Yonkee and Weil, 2015), grains of this age range should be sparse in the DZ age spectra.

Sources of Laramide-Age (ca. 80–50 Ma) Zircons

Potential source regions of Laramide (ca. 80–50 Ma) ages present in the DZ age spectra of the SJB include the North American porphyry copper province of southern Arizona, southwestern New Mexico, and northern Sonora and the Colorado mineral belt, a linear belt of laccolithic-plutonic-volcanic complexes stretching from south-central Colorado into far northeastern Arizona (Figs. 1 and 6; Table 2).

In the Laramide porphyry copper province south of the SJB, various Laramide-age volcanic and plutonic rocks are as old as ca. 80–76 Ma (Ramos-Velázquez et al., 2008). However, most of the mineralizing porphyries in this region were emplaced in the ca. 75–52 Ma range (Seedorff et al., 2005; Valencia et al., 2005; Valencia et al., 2006; Ramos-Velázquez et al., 2008; González-León et al., 2011; Leveille and Stegen, 2012; Mizer, 2013; Vickre et al., 2014; Favorito and Seedorff, 2017). A potential sampling bias exists because the majority of the U-Pb age dating on the porphyry copper systems has been focused on the mineralizing porphyries and their host rocks, and because the Laramide volcanic carapaces to these systems have been largely removed by erosion. However, we can still characterize the main age bracket for southern Arizona at ca. 75–55 Ma, southwestern New Mexico at ca. 64–55 Ma, and northern Sonora at ca. 80–50 Ma. These age ranges indicate a general younging from west to east as Laramide deformation and magmatism migrated eastward toward the interior of the continent (Leveille and Stegen, 2012).

The Coastal Sonoran Batholith west of Hermosillo, Sonora experienced Laramide magmatism ranging from ca. 80 to 69 Ma (Ramos-Velázquez et al., 2008). Farther inland in Sonora, the Tarahumara assemblage and associated Laramide plutonic rocks of northern Sonora span the interval from ca. 76 to 50 Ma (González-León et al., 2011), including Laramide porphyry copper deposits at Cananea and Nacozari at ca. 64 Ma and ca. 56–52 Ma, respectively (Valencia et al., 2005; Valencia et al., 2006). However, these regions lie >500 km south of the SJB and are on the opposite side of the inferred and inverted Border Rift system divide present in southeastern Arizona and northern Sonora (Lawton and Bradford, 2011), making it unlikely that detritus from northern Sonora was transported to the SJB by either fluvial or eolian transport.

Plutonic activity in the Colorado mineral belt has been well documented by K-Ar, Ar-Ar, and zircon fission-track analyses to the age ranges of ca. 75–65 Ma and ca. 35–23 Ma (Armstrong, 1969; Cunningham et al., 1994; Mutschler et al., 1997; Semken and McIntosh, 1997; Chapin et al., 2004; Chapin, 2012; Gonzales, 2015). However, these methods and results are not directly comparable to U-Pb zircon ages, so are not considered in the provenance assessment of SJB strata. A limited number of U-Pb zircon geochronologic analyses on Colorado mineral belt plutons and laccoliths are reported in Gonzales (2015) and are summarized in Table 2. Magmatic activity in the Ouray, Colorado region of the San Juan Mountains falls in the age range of ca. 69–57 Ma (Gonzales, 2015). Plutonic activity in the La Plata Mountain region of the Colorado mineral belt occurred in the age range of ca. 70–57 Ma (Gonzales, 2015).

Although each of these regions experienced magmatism during distinct intervals, there is a large degree of zircon age overlap between the southwestern part of the North American porphyry copper province and the Colorado mineral belt. Therefore, source areas of Laramide DZ in SJB strata cannot be distinguished on DZ ages alone.

DZ Grain Age Analysis—Changing Proportions of <285 Ma Grains throughout SJB Strata

Tables 3A and 3B show the general pattern of DZ grains in SJB strata that are <285 Ma. These grains must have been derived from Cordilleran arc magmatism to the north, west, and south, including rocks formed in an easterly sweep of magmatism that includes the Colorado mineral belt. We do not further consider grain ages forming ≤5% of arc-derived grains <285 Ma.

TABLE 2. U-Pb COMPILATION OF POTENTIAL LARAMIDE-AGE (CA. 80–50 MA) SOURCES: SOUTHWESTERN NORTH AMERICA LARAMIDE PORPHYRY COPPER PROVINCE (LPCP) IN SOUTHERN ARIZONA, SOUTHWESTERN NEW MEXICO, AND NORTHERN SONORA, MEXICO AND COLORADO MINERAL BELT (CMB), SOUTHWESTERN COLORADO AND NORTHEASTERN ARIZONA

Region	Location	Approximate U-Pb age range (Ma)	U-Pb reference
Southwestern North America Laramide Porphyry Copper Province (LPCP)			
LPCP in southern Arizona (ca. 74–52 Ma)	Various deposits Globe-Miami, Superior, Ray, Arizona	75–61	Seedorff et al., 2005
	Various locations throughout Arizona	76–54	Leveille and Stegen, 2012
	Patagonia Mountains, Santa Cruz County, Arizona	74–56	Vickre et al., 2014
	Tortilla Mountains, Pinal County, Arizona	70–66	Favorito and Seedorff, 2017
LPCP in southwestern New Mexico (ca. 75–55 Ma)	Various locations throughout New Mexico	60–55	Leveille and Stegen, 2012
	Silver City, Central Mining District, New Mexico	64–55	Mizer, 2013
LPCP in northern Sonora (ca. 80–50 Ma)	La Caridad mine, Nacozari, Sonora	56–52	Valencia et al., 2005
	Milpillas mine, Cananea District, Sonora	64	Valencia et al., 2006
	Coastal Sonoran Batholith, west of Hermosillo, Sonora	80–69	Ramos-Velázquez et al., 2008
	Sonoran Batholith near Arizpe, Sonora	76–50	González-León et al., 2011
Colorado mineral belt (CMB), southwestern Colorado and northeastern Arizona			
CMB: Ouray, San Juan Mountains, Colorado (ca. 69–57 Ma)	Oak Creek, Ouray area, Colorado	65–64	Gonzales, 2015
	The Blowout, Ouray area, Colorado	66–65	
	Coal Back Pass, Rico, Colorado	69–65	
	Hermosa Peak, Rico, Colorado	68–57	
CMB: La Plata Mountains, Colorado (ca. 70–57 Ma)	The Notch, La Plata Mountains, Colorado	70–69	Gonzales, 2015
	Sleeping Ute Mountain, La Plata Mountains, Colorado	68–57	

Figure 7 displays the (<285 Ma) DZ age distribution and the biostratigraphic age range based on ammonite zones (Nummedal, 2004) for each unit sampled in the SJB. The results indicate a strong overlap between detrital-zircon peak ages from the combined probability distribution plots and biostratigraphic ages, beginning with the Gallup Sandstone and continuing up-section through the San Jose Formation. All but three newly reported individual samples overlap maximum depositional age weighted averages (Table 1) with biostratigraphic ages within uncertainty (2 sigma); the exceptions are two Lewis Shale samples (WP61 and WP62), which were likely affected by longshore currents that potentially homogenized the DZ age distribution, and one Cliff House Sandstone sample (WP41). This overlap between depositional ages and detrital-zircon crystallization ages means the source to sink transport of these approximately depositional-age zircons must have occurred rapidly over the course of 1–2 m.y., either by fluvial transport or airfall.

In four pre–Lewis Shale (>75 Ma depositional-age) samples, 55%–75% of arc-derived grains <285 Ma are Jurassic or Permian–Triassic and were likely derived from the pre–Laramide arc assemblage lying generally south of the international border but also extending northwestward into the Mojave region (a lesser 25%–45% of Cretaceous arc-derived grains in the same samples were presumably derived from younger components of that arc assemblage).

In four post–Cliff House (<75 Ma depositional-age) Campanian samples, the proportion of combined Jurassic and Permian–Triassic grains in the arc-derived (<285 Ma) population is only 20%–35%, suggesting that the pre–Laramide arc to the south and southwest had by then been overprinted by Cretaceous arc rocks (Laramide porphyry copper province), and/or another provenance (Colorado mineral belt) had come into play.

In the Maastrichtian McDermott Formation sample, the proportion of Laramide-age grains (ca. 75–65 Ma) is >90%, with no other <285 Ma age bracket represented by more than 5% of <285 Ma grains. If Colorado mineral belt sources are significant for the SJB, they are most likely in the McDermott Formation, which is consistent with McDermott and Animas paleoflow indicators. More than three-quarters of the Laramide-age (ca. 75–65 Ma) grains in the McDermott Formation sample could have been derived from the nearby ca. 70–57 Ma San Juan and/or La Plata laccoliths (Gonzales, 2015) as Laramide deformation got under way near the SJB. Other likely sources of these Laramide-age grains are the Ouray and Rico intrusive centers. An intriguing aspect of these two Colorado mineral belt intrusive centers is that the La Plata Mountains, Sleeping Ute, and Lone Cone laccoliths contain an inordinately high proportion of Proterozoic xenocrysts and very few zircons yielding Laramide crystallization ages, whereas the nearby San Juan intrusive rocks contain abundant zircons that grew during Laramide emplacement, some of

TABLE 3A. <75 MA PROPORTIONS OF ARC-DERIVED <285 MA GRAINS IN SAN JUAN BASIN STRATA

Unit	Depositional age (Ma)	Total no. DZ grains	No. Arc DZ grains	Arc DZ Grains (%)	Arc DZ grains (%) 60–65 Ma	65–70 Ma	70–75 Ma
San Jose	55–50	188	31	16	0	5	11
Nacimiento	65–61	177	60	34	3	14	31
Animas	66–60	299	101	36	35	32	14
Ojo Alamo	66–65	297	0	24	N/A	4	17
McDermott	68–67	186	86	46	N/A	77	15
Kirtland	74–71.5	276	119	25	2	10	37
Fruitland	75.5–73.5	196	97	49	N/A	10	50
Pictured Cliffs	80.5–74.5	177	73	41	N/A	N/A	8
Lewis	80.5–74.5	294	38	13	N/A	N/A	22
Cliff House	80.5–79.5	196	48	24	N/A	N/A	N/A
Menefee	85–78.5	117	59	50	N/A	N/A	N/A
Point Lookout	85–80.5	196	53	27	N/A	N/A	N/A
Gallup	91–88.5	87	13	15	N/A	N/A	N/A

TABLE 3B. >75 MA PROPORTIONS OF ARC-DERIVED <285 MA GRAINS IN SAN JUAN BASIN STRATA

Unit	Depositional age (Ma)	Percentages of arc DZ grains 75–80 Ma	80–90 Ma	90–100 Ma	101–145 Ma	145–201 Ma	202–284 Ma
San Jose	55–50	13	13	13	3	26	16
Nacimiento	65–61	8	5	2	3	22	12
Animas	66–60	2	2	1	1	9	3
Ojo Alamo	66–65	3	0	9	0	39	29
McDermott	68–67	1	1	0	0	5	1
Kirtland	74–71.5	11	2	3	4	21	10
Fruitland	75.5–73.5	16	3	1	0	12	8
Pictured Cliffs	80.5–74.5	32	5	14	7	27	7
Lewis	80.5–74.5	13	13	10	8	24	10
Cliff House	80.5–79.5	8	5	15	14	38	21
Menefee	85–78.5	2	5	10	7	36	41
Point Lookout	85–80.5	2	21	13	8	49	6
Gallup	91–88.5	N/A	N/A	23	8	54	15

Note: Depositional ages are taken from ammonite zones (Nummedal, 2004, Fig. 6) and Cather (2004, Fig. 2 and Table 1) as calibrated by Gradstein et al. (2012) [GSL 2012/GSA 2013 timescale]. N/A denotes impossible or implausible grain ages (depositional age older than grain age range). DZ—detrital zircon.

which have inherited Proterozoic cores (Gonzales, 2015). These are nuances that are yet to be fully understood but may indicate the Laramide-age zircons in the McDermott and Animas Formations were likely derived from either the volcanic cover that may have existed over the Rico intrusive center or from another nearby intrusive center such as Ouray.

Although paleoflow was from the northwest (Klute, 1986) or north (Sikkink, 1987), the Ojo Alamo grain population <285 Ma consists of 68% Jurassic plus Permian–Triassic grains and only 21% Laramide (<75 Ma) grains, compared to ~80% Laramide-age grains in the McDermott Formation. Detrital-sanidine Ar-Ar ages confirm the Ojo Alamo Sandstone was deposited ca. 65.6 Ma (Pappe et al., 2013). Only five (indicated in Supplemental Item 2 [footnote 2], Ojo Alamo composite tab) of the 295 U-Pb DZ ages from the Ojo Alamo Sandstone overlap the biostratigraphic age. The paucity of depositional-age grains suggests that the Ojo Alamo Sandstone was largely derived from reworking of Jurassic and Cretaceous cover. This interpretation is consistent with the notion that the McDermott Formation and Ojo Alamo Sandstone are likely proximal versus distal facies of approximately the same age, where detrital zircons in the Ojo Alamo Sandstone could have been largely recycled from Jurassic and Cretaceous cover over the La Plata laccoliths as they were unroofed during Laramide deformation and a combination of reworked Jurassic and Cretaceous strata plus Colorado mineral Belt volcanic sources for McDermott sedimentation.

Both McDermott and Animas Formations contain (in their <285 Ma grain populations) ~80% Laramide-age grains that, given southeasterly-directed paleocurrents, were likely derived from Colorado mineral belt laccoliths, with only 6%–12% Jurassic plus Permian–Triassic grains that could well have been recycled from older Mesozoic strata exposed near the laccoliths and/or plutons in Laramide time. The Animas Formation from the northern part of the SJB and in the San Juan sag across the Archuleta anticlinorium contains by far the highest proportion (35%) of <65 Ma grains among its <285 Ma grains. The geography seems suitable for derivation from the northeastern-most (Rico–San Miguel–Ouray) laccoliths and/or plutons (ca. 70–57 Ma) of the igneous clusters that form the southwestern end of the Colorado mineral belt and/or from igneous sources in the Twin Lakes batholith of the Sawatch Range to the north that had a pulse of felsic magmatism ca. 64–54 Ma (Feldman, 2010).

The Nacimiento Formation contains <50% of Laramide-age (<65 Ma) grains in its <285 Ma grain population, coupled with nearly as many (36%) older Jurassic plus Permian–Triassic grains. Thus, in Paleocene time, most of the sediment entering the SJB was being generated from erosion of nearby Laramide basement block uplifts and their overlapping sedimentary cover. The San Jose Formation displays a mixed age signature, containing only 16% Laramide (ca. 75–65 Ma) grains and 42% Jurassic plus Permian–Triassic grains. Based on a strong southeasterly paleoflow, it is likely the sediments contained in the San Jose Formation were derived from bedrock sources or were recycled from older strata as Laramide uplifts formed. The similarities in DZ age distributions between the San Jose Formation, Nacimiento Formation, and the Ojo Alamo Formation are striking in both the <285 Ma range (Fig. 7), as well as the entire 0–3250 Ma range (Fig. 5), which is not surprising based on the notion these are the three units that are mainly derived from reworking of the Mesozoic and early Cenozoic cratonal blanket.

PROVENANCE ASSESSMENT

Changes in Sediment Provenance

Three distinct changes in sediment provenance are evident in the detrital record of Cretaceous and younger sediments of the SJB (Figs. 7 and 8). The first provenance change occurs between the Lower Cretaceous Burro Canyon Formation and the overlying Gallup Sandstone and Lewis Shale and is identified by the addition of ca. <100 Ma grains and a decrease in peri-Gondwanan (ca. 750–550 Ma) grain ages. This initial transition is interpreted to reflect the introduction of sediment from the Mogollon highlands and decreasing sediment input from the Sevier thrust belt. The second change in provenance occurs between the Lewis Shale and the overlying Pictured Cliffs Sandstone and is indicated by the addition of abundant Laramide-age grains (ca. 75 Ma). This transition reflects sediment derivation directly from the Laramide porphyry copper province of southern Arizona and southwestern New Mexico. The third provenance shift occurs at the base of the Kirtland Formation with the disappearance of Archean, Neoproterozoic, and Paleozoic grains. This third transition is interpreted to reflect major drainage reorganization due to developing Laramide basement uplifts, including unroofing of the adjacent San Juan and Nacimiento uplifts.

Molenaar (1977) recognized a change in sediment source area within the uppermost Kirtland Shale and attributed this change to the initiation of igneous activity in the Four Corners region during the Late Cretaceous. Petrologic and paleoflow evidence supports this provenance interpretation, indicating that the source was likely to the north or northwest, and erosion of these grains results from the unroofing of Precambrian rocks of the Needle Mountains uplift in southwestern Colorado (Powell, 1972; Klute, 1986). Cather (2004) indicates the earliest occurrence of detritus from Paleozoic and Precambrian sources was ca. 65 Ma with the deposition of the Ojo Alamo Sandstone, but our new DZ results suggest this change actually occurs in the upper Kirtland Formation. These results also support the argument of Cather (2004) that the initiation of Laramide tectonism and rapid subsidence in the SJB preceded deposition of the Ojo Alamo Sandstone by ~15 m.y. Emplacement of the Laramide plutons and laccoliths contributed >1 km to the elevation of the region, resulting in a generally southward drainage system in the southern SJB (Gonzales, 2015; Donahue, 2016).

Provenance Intervals

Based on DZ ages, the SJB can be divided into four stratigraphic intervals (Fig. 8) that display internally consistent age peaks: (1) Lower Cretaceous Burro Canyon Formation, (2) Turonian Gallup Sandstone through Campanian Lewis Shale, (3) Campanian Pictured Cliffs Sandstone through Fruitland Formation, and (4) Campanian Kirtland Sandstone through Eocene San Jose Formation. Combining multiple samples into composite DZ age spectra highlights clear differences between the four intervals (Fig. 8). These composite DZ age spectra from our new data allow comparisons with existing composite DZ references (e.g., Dickinson et al., 2012), bolster the number of U-Pb analyses per group, paralleling the large-n analysis routine described in Pullen et al. (2014), minimize "noise" in the age spectra that result in smoother probability density plot curves, and allow for evaluation of relative proportions of various age peaks, not just their presence or absence (Pullen et al., 2014).

1. Lower Cretaceous Burro Canyon Formation

Based on petrofacies and DZ age signature reported in Dickinson and Gehrels (2008), the Jackpile Sandstone (CP53, used in this study) is correlated with Cedar Mountain–Burro Canyon samples and reported herein as such. A composite probability density plot composed of two samples from the Lower Cretaceous Burro Canyon Formation (CP27 and CP53) yields a complex spectrum of ages with numerous age peaks (Fig. 8). This spectrum contains Archean ages ranging from ca. 3100 to 2600 Ma, Proterozoic ages ranging from ca. 1950 to 542 Ma, Paleozoic ages ranging from ca. 500 to 275 Ma, and Mesozoic ages ranging from ca. 245 to 150 Ma.

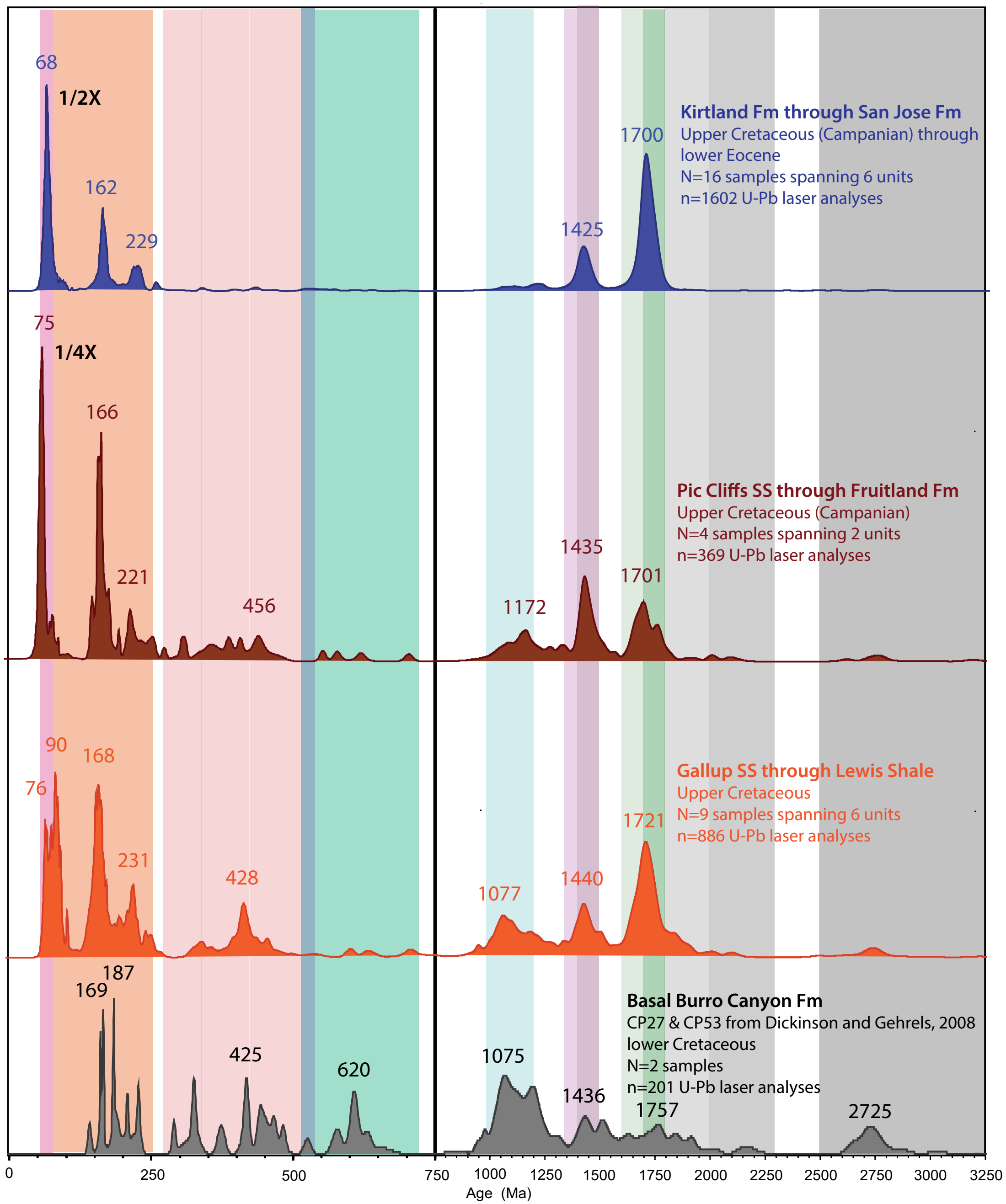

Figure 8. Normalized age distribution curves of composite detrital-zircon (DZ) samples (0–3250 Ma). Samples from contiguous units with similar DZ age distributions and similar paleocurrent flow are grouped together resulting in the four composite groupings shown. Samples are stacked from oldest (Burro Canyon Formation) to youngest (Kirtland Formation through San Jose Formation). N is the number of samples composited, and n is the total number of DZ ages in each composited distribution. Colored bands (A–M) correspond to the North American crustal province map (Fig. 6). 0–750 Ma scale is expanded to show the young end of the age spectra in greater detail. The bold "1/2x" and "1/4x" mean the tallest peaks from those particular age spectra have been reduced by 50% and 75% in height, respectively. This was done to enhance the other age peaks that would be diminished otherwise.

Dickinson and Gehrels (2008) inferred that the Cedar Mountain Formation (proximal equivalent of the Burro Canyon Formation) was derived from the Sevier thrust front, and Burro Canyon Formation proper was derived from the Mogollon highlands. However, direct comparison to the southern Sevier reference-subset J and the northern Sevier reference-subset I from Dickinson et al. (2012) suggests these samples from the Lower Cretaceous basal Burro Canyon Formation have provenance ties to the Sevier retroarc fold-and-thrust belt to the west (Fig. 9). Derivation of the Burro Canyon Formation from sources exposed within the Sevier thrust belt is consistent with a Lower Cretaceous paleoflow direction toward the east and northeast (Dickinson and Gehrels, 2008, their figure 5). The Burro Canyon Formation also contains abundant ages ranging from 650 to 570 Ma, indicative of peri-Gondwanan derivation (Dickinson and Gehrels, 2009a). All of these lines of evidence support the interpretation that the Burro Canyon Formation sediments were derived directly from the eroding Sevier retroarc fold-and-thrust belt to the west and/or partial recycling of Colorado Plateau sediments including the Jurassic eolianites (Dickinson and Gehrels, 2008, 2009b).

2. Turonian Gallup Sandstone through Campanian Lewis Shale

We compile nine samples spanning six units from the Gallup Sandstone through the Lewis Shale into one composite probability density plot consisting of 891 U-Pb zircon ages and dominated by Paleoproterozoic and Mesoproterozoic ages ranging from ca. 1950 to 1600 Ma and ca. 1550 to 1000 Ma (Fig. 8). This composite plot contains a few scattered Neoproterozoic ages ranging from ca. 700 to 550 Ma and a significant number of Paleozoic ages ranging from ca. 500 to 290 Ma. This sequence also contains a significant proportion (23%) of Mesozoic zircons ranging in age from ca. 250 to 73 Ma.

Direct comparison to the Sevier and Mogollon reference-subset K from Dickinson et al. (2012) suggests the Gallup Sandstone through Lewis Shale interval has provenance ties to both the Sevier fold-and-thrust belt to the west and the Mogollon highlands rift shoulder to the southwest (Fig. 10). This interval likely represents reworking of the sedimentary cover that was being shed from both of these high-standing structural features. Triassic and Jurassic DZ grains could be transported directly west from the Cordilleran arc via fluvial transport, but the preservation of Grenville- and Appalachian- (Taconic and Acadian) derived zircons present in Paleozoic strata of the Colorado Plateau (Gehrels et al., 2011) suggest that it is more likely these Triassic and Jurassic detrital zircons also represent reworking of the Mesozoic sedimentary blanket of the region.

3. Campanian Pictured Cliffs Sandstone through Fruitland Formation

A total of 373 U-Pb laser analyses from four samples of Pictured Cliffs Sandstone and the Fruitland Formation yield results very similar to the Gallup Sandstone through Lewis Shale section (Fig. 8), with the main difference in the influx of near-depositional-age zircons (main age peak at 75 Ma) preserved in the younger section. This interval also likely represents reworking of the Late Cretaceous sedimentary cover that was still being eroded from both the Sevier

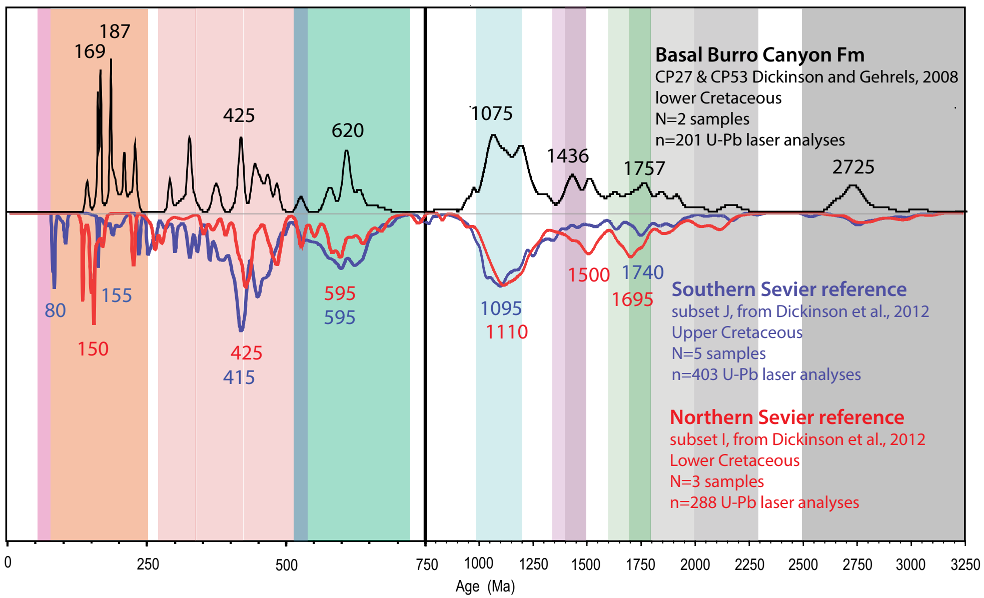

Figure 9. Normalized age distribution curves of composite detrital-zircon (DZ) samples (0–3250 Ma). N is the number of samples composited, and n is the total number of DZ ages in each composited distribution. Colored bands (A–M) correspond to the North American crustal province map (Fig. 5). 0–750 Ma scale is expanded to show the young end of the age spectra in greater detail.

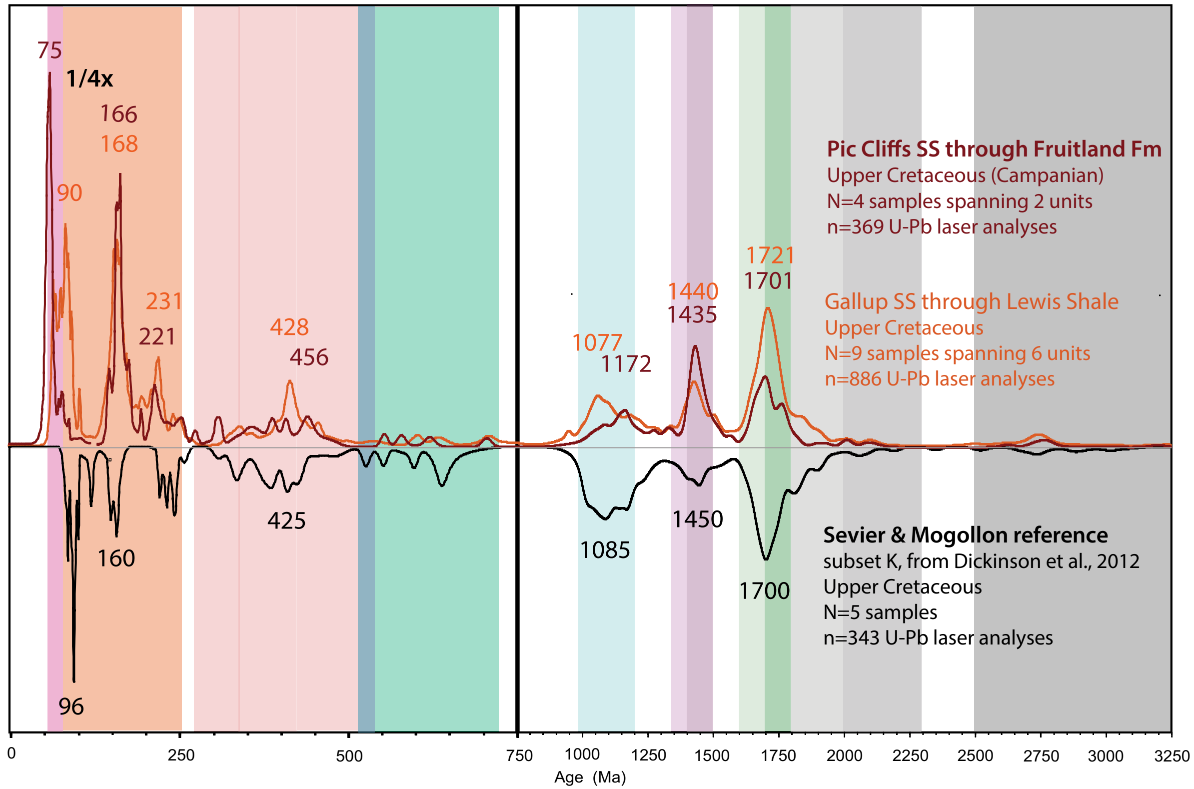

Figure 10. Normalized age distribution curves of composite detrital-zircon (DZ) samples (0–3250 Ma). N is the number of samples composited, and n is the total number of DZ ages in each composited distribution. Colored bands (A–M) correspond to the North American crustal province map (Fig. 6). 0–750 Ma scale is expanded to show the young end of the age spectra in greater detail. The bold "1/4x" means the tallest peak has been reduced by 75% in height to enhance the other age peaks that would be diminished otherwise.

fold-and-thrust belt, in addition to the Mogollon highlands region (Fig. 10). This interval also contains the pervasive Grenville ages (ca. 1200–1000 Ma) that are present in all units from the Basal Burro Canyon through the Fruitland Formation. The Fruitland Formation is also the youngest SJB unit that contains a significant fraction of Paleozoic (ca. 500–290 Ma) grains, which were also derived from reworking the Paleozoic section of the Colorado Plateau but were originally sourced from the Appalachian region (Gehrels et al., 2011).

The Pictured Cliffs Sandstone through Fruitland Formation interval contains a significant proportion (34%) of Cretaceous zircons. Based on paleocurrent indicators within both units, these zircons were likely derived from the Laramide porphyry copper province in southern Arizona and/or southwestern New Mexico. The timing of the influx of near-depositional-age grains (ca. 77–75 Ma) matches closely with the time frame (ca. 76–75 Ma) that Liu et al.'s (2010) reconstruction locates the Shatsky conjugate under the Four Corners region, setting the stage for the Laramide block uplifts and a change in local drainage patterns. However, Heller et al. (2013) show the Shatsky conjugate beneath Four Corners during Ojo Alamo Sandstone deposition at ca. 65 Ma. While it is uncertain what the upper-crustal response was at the moment the proposed Shatsky conjugate passed under the SJB region, our new DZ data are more consistent with the Liu et al. (2010) model, in which the Shatsky conjugate was under the SJB region at ca. 76 Ma, immediately preceding deposition of the Kirtland Formation (ca. 74.6–72.8 Ma; $^{40}Ar/^{39}Ar$ ages of ash beds in the Kirtland Formation are reported in Fassett and Steiner, 1997; Sullivan and Lucas, 2006).

4. Campanian Kirtland Sandstone through Eocene San Jose Formation

A composite age distribution of 1602 U-Pb ages from 16 Upper Cretaceous Kirtland Sandstone through Lower Eocene San Jose Formation samples yields a strikingly simple age curve consisting of five discrete age peaks (Figs. 8 and 11). The age spectra from this interval are dominated by Paleoproterozoic (ca. 1800–1600 Ma) and Mesoproterozoic (ca. 1500–1000 Ma) zircons, and these units also contain abundant Mesozoic zircons ranging in age from ca. 250 to 66 Ma.

The time interval represented by the Campanian Kirtland Formation through Eocene San Jose Formation records a profound increase in the pro-

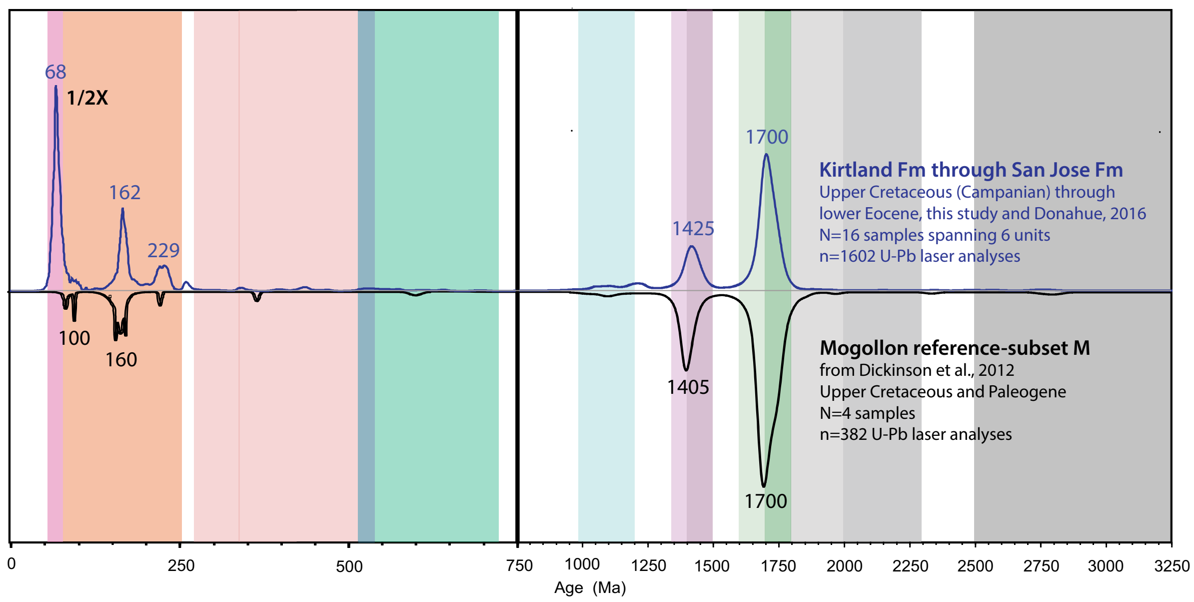

Figure 11. Normalized age distribution curves of composite detrital-zircon (DZ) samples (0–3250 Ma). N is the number of samples composited, and n is the total number of DZ ages in each composited distribution. Colored bands (A–M) correspond to the North American crustal province map (Fig. 6). 0–750 Ma scale is expanded to show the young end of the age spectra in greater detail. The bold "1/2x" means the tallest peak has been reduced by 50% in height to enhance the other age peaks that would be diminished otherwise.

portion of Paleoproterozoic (ca. 1800–1600 Ma) grains and a significant decrease in the number of Grenville-age (ca. 1200–1000 Ma) grains. This likely represents a shift from sediment derivation primarily from the Sevier and Mogollon regions, as demonstrated for the Gallup Sandstone through Fruitland Formation, to predominantly locally derived sediment shed directly from the surrounding Laramide basement-cored uplifts, which were tectonically active during this time interval (Cather, 2004). Comparing reference-subset M (Dickinson et al., 2012), a proxy for the DZ signature that would be derived from the erosion of the Cretaceous sedimentary cover over the local basement core uplifts, with the age spectra produced from Kirtland Formation through San Jose Formation (Fig. 11) results in an almost perfect match of age ranges and peaks, except for the youngest age peak (68 Ma) that represents Colorado mineral belt derivation. This distinctive shift from distal to proximal sediment sources has also been documented in Maastrichtian (ca. 70 Ma) time within the Raton basin, which lies to the east of the SJB (Bush et al., 2016).

The pervasive Triassic (ca. 235–215 Ma) and Jurassic (ca. 190–155 Ma) signatures in the DZ age spectra throughout all four provenance intervals could only be derived from two sources: (1) directly from the Triassic–Jurassic magmatic arc that was situated along the western margin of North America or (2) reworked through the Mesozoic eolianites and sedimentary blanket that once covered most of the Colorado Plateau region. Based on the dominant paleocurrent directions and the estimated thickness of eroded Mesozoic and early Cenozoic sedimentary cover, we conclude that erosion and redeposition of the Triassic–Jurassic and younger sediments are the main drivers for at least the Upper Cretaceous and Eocene units. As the surrounding Laramide blocks were uplifted and eroded, the sedimentary cover would provide the first sediment into the SJB, with increased Precambrian grains as the Proterozoic crystalline basement rocks were further exhumed.

Samples from the Kirtland, McDermott, and Animas Formations contain depositional-age zircons that likely originated from either the Laramide porphyry copper province of southeastern Arizona, southwestern New Mexico, and northern Sonora, or the nearby Colorado mineral belt to the north-northwest. The abrupt change in paleocurrent directions, from trending toward the northeast to trending toward the south-southwest, beginning with the Paleocene Ojo Alamo Sandstone and continuing through the McDermott and Animas Formations, indicates that the likely source of depositional-age grains was the neighboring Colorado mineral belt.

Paleo-Drainage Interpretation

From ca. 125 to 75 Ma, sediments derived from both the high-standing Sevier thrust front (Nevadaplano) and the Mogollon highlands were deposited in the broad foreland basin that occupied the greater Four Corners region (Dickinson and Gehrels, 2008; Lawton and Bradford, 2011; Dickinson et al., 2012). However, beginning ca. 75 Ma, Laramide block uplifts had a profound effect on the geomorphology of the Four Corners region, partitioning this once continuous foreland basin into smaller isolated intra-foreland basins typically surrounded by basement-cored uplifts (Fig. 12). As Laramide thrusts generated

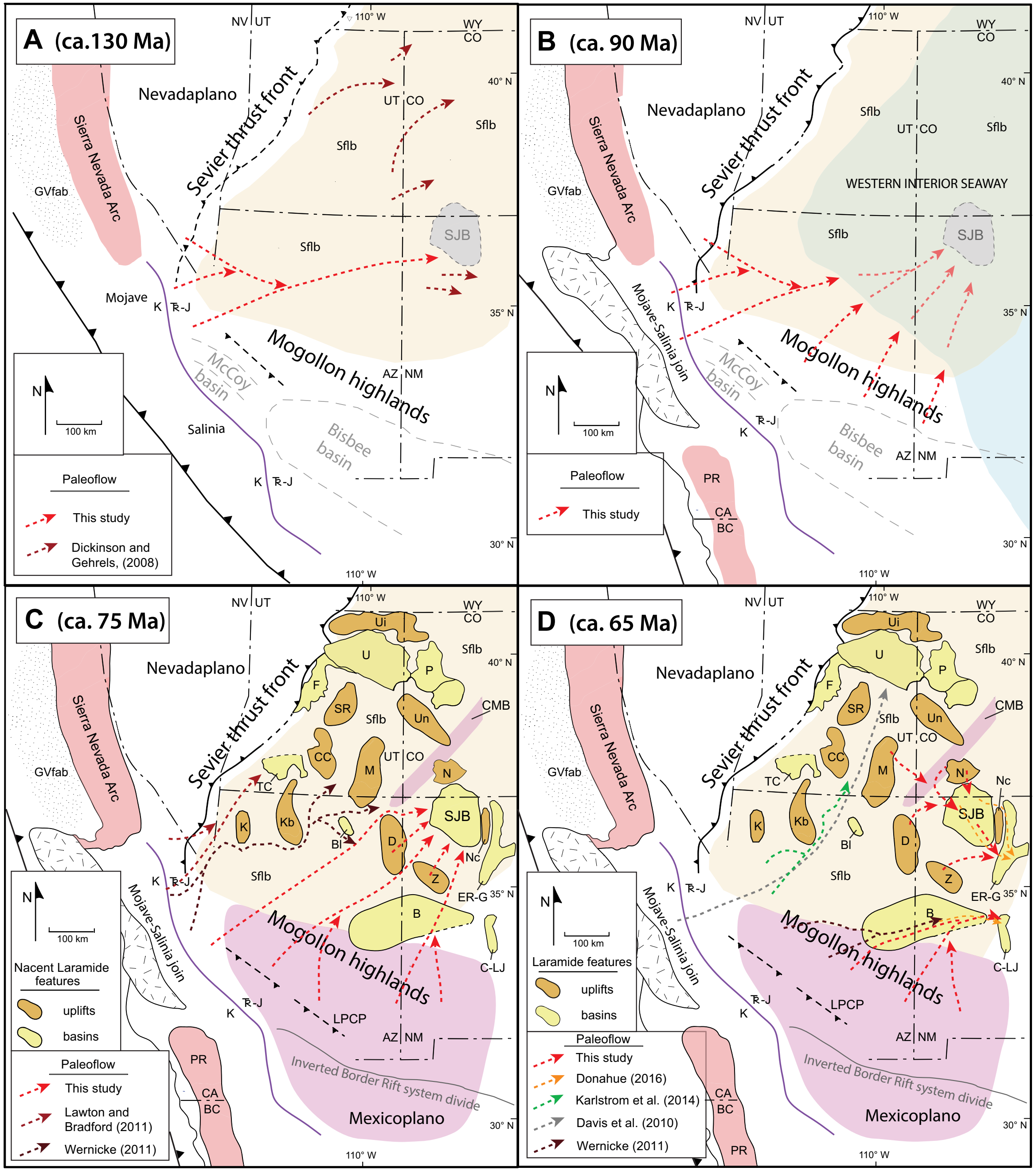

Figure 12. Paleogeographic maps of the Four Corners region in relationship to Cordilleran tectonic features. Figure entails four discrete timeframes: (A) ca. 130–125 Ma, Barremian–Aptian (Jurassic) corresponds with deposition of the Burro Canyon Formation (Dickinson and Gehrels, 2008); (B) ca. 90–88 Ma, Turonian (Upper Cretaceous) corresponds with deposition of the beach sand Gallup Sandstone; (C) ca. 75–73 Ma, Late Campanian (Upper Cretaceous) corresponds with the early phases of Laramide tectonism and deposition of the time-transgressive stratigraphy from Lewis Shale through Fruitland Formation; (D) ca. 65–62 Ma, Early Paleocene corresponds to deposition of the Ojo Alamo Sandstone, Nacimiento Formation, and Animas Formation. Figures have been restored palinspastically after Dickinson (2011), and modified from Blakey (2012) and Dickinson et al. (2012). Laramide basins (Maastrichtian–Paleogene sediment fill) after Lawton (2008) and Cather (2004): SJB—San Juan; B—Baca; BI—Black Mesa; C-LJ—Carthage-La Joya; ER-G—El Rito–Galisteo; TC—Table Cliff; P—Piceance; U—Uinta; F—Flagstaff. Laramide uplifts after Kelley (1955): Nc—Nacimiento; D—Defiance; N—Needle Mountains (San Juan); Kb—Kaibab; K—Kingman; M—Monument; CC—Circle Cliffs; SR—San Rafael; Ui—Uinta; Un—Uncompahgre; Z—Zuni. Proposed paleorivers are represented with dashed lines with arrows: red—this study; brown—Lawton and Bradford (2011); gray—Davis et al. (2010); black—Wernicke (2011); green—Karlstrom et al. (2014). State boundaries are dash-dot-dash lines: UT—Utah; CO—Colorado; AZ—Arizona; NM—New Mexico; NV—Nevada; CA—California; BC—Baja California. Nevadaplano after DeCelles (2004). Purple line is approximate boundary between Triassic–Jurassic (TR-J) and Cretaceous (K) arc magmatism (Dickinson et al., 2012). Sflb—Sevier Foreland Basin; LPCP—Laramide porphyry copper province; CMB—Colorado mineral belt magmatism. Location of inverted Border Rift System divide from Lawton and Bradford (2011).

topographic relief and adjacent depositional centers (i.e., SJB), erosion of the cratonal blanket provided the initial sediment into the SJB, followed by subsequent exhumation of cratonal basement sources. These reworked sediments were most likely the source for much of the sediments seen in the SJB beginning in Late Campanian time and continuing into the Eocene.

During most of late Mesozoic time, drainage systems in the Four Corners region flowed toward the northeast. During this time, sediment delivery to the region was primarily being generated from the distant Mogollon highlands and Sevier thrust front (Fig. 12B). In the Farmington region, thickening of the Campanian Kirtland Formation (ca. 74–71 Ma) indicates the bordering Hogback monocline was active during Kirtland deposition, as Laramide orogenesis began to shape the local landscape, and alter paleodrainage patterns (figure 22 from Cather, 2004). Paleocurrent indicators in the Kirtland Formation (Fig. 4) provide the earliest evidence that paleoflow was shifting from northeast directed to east directed (Fig. 12C). The DZ age spectra from the Kirtland Formation indicate a change in sediment provenance ca. 73 Ma, which matches well with the shift in Kirtland paleoflow. However, it wasn't until deposition of the fluvial Ojo Alamo Sandstone that the paleoflow fully shifted to be south-southeast directed (Fig. 12D). This south-southeast–directed paleoflow persisted through the Paleocene and into the Eocene, evidenced by paleoflow indicators in the Nacimiento and San Jose Formations, respectively.

CONCLUSIONS

Cretaceous through mid-Paleogene strata of the Four Corners region provide an excellent opportunity to decipher changes in sediment provenance during the transition from Sevier thin-skinned thrusting through the formation of regional Laramide basement uplifts. DZ age spectra, in conjunction with paleocurrent data, reveal three distinct changes in sediment provenance during Cretaceous–Early Eocene time; these changes define four stratigraphic intervals with internally consistent age distributions. Comparison of each stratigraphic interval with reference DZ data sets supports the following model: (1) During Early Cretaceous time, sediment was entering the Four Corners region predominantly from the Sevier thrust front, as uplifted Paleozoic and Mesozoic passive margin sediments were eroded; (2) during Turonian and Coniacian time (93.9–86.3 Ma), the Four Corners region was receiving sediment from both the Sevier thrust belt to the west and the Mogollon highlands rift shoulder to the south-southwest, but relative proportions of each are unknown; and (3) during the Laramide orogeny (ca. 75–55 Ma), deformation migrated eastward toward the interior or North America, which created differential subsidence and sedimentation. The SJB sediments were derived predominantly from the surrounding fault-bounded Precambrian basement-block uplifts and their sedimentary cover, in addition to input from the nearby Colorado mineral belt.

Two possible sources of the abundant Laramide-age grains in the SJB include: (1) the porphyry copper province of southern Arizona, southwestern New Mexico, and northern Sonora, and (2) the Colorado mineral belt predominantly in extreme southwestern Colorado. While there is significant age overlap in the two regions, DZ results and paleoflow indicators suggest derivation from the south-southwest porphyry copper province (in southern Arizona and/or southwestern New Mexico) during deposition of the Pictured Cliffs Sandstone and Fruitland Formation (ca. 76–73 Ma), followed by derivation from the Colorado mineral belt from uplifted basement blocks to the NNW beginning with the Kirtland Formation, beginning ca. 73 Ma. The timing of this provenance change matches well with the model of Liu et al. (2010), which places the Shatsky conjugate under the SJB region at the same time, indicating plate interactions at depth may be the driver of the tectonics our DZ age spectra record. Overall, the DZ age spectra in the SJB document the transition from initial reworking of the Paleozoic and Mesozoic cratonal blanket to unroofing of basement-cored uplifts and Laramide plutonic rocks with the Campanian onset of Laramide deformation in the Four Corners region.

ACKNOWLEDGMENTS

We would like to acknowledge ExxonMobil Upstream Research for their generous financial support of this project and the Convergent Orogenic Systems Analysis (COSA) collaboration with the University of Arizona Department of Geosciences. We thank Steve May and Steve Cather for their critical insights into the San Juan Basin geology and also recognize the National Science Foundation (NSF grant EAR-1649254) for their continued support of the Arizona LaserChron Center. Roswell Juan, John Yang, Kenneth Kanipe, and Gayland Simpson provided important technical support in preparing the zircon heavy-mineral separates, as did Clayton Loehn for his assistance acquiring the scanning electron microscope images of the zircons. We are grateful to Nicky Giesler and Chelsi White for their assistance in preparing the mounts and countless hours spent acquiring the analytical data. We finally thank Kathleen Surpless and an anonymous reviewer who provided exceptionally thorough and helpful reviews of this manuscript.

REFERENCES CITED

Armstrong, R.L., 1968, Sevier orogenic belt in Nevada and Utah: Geological Society of America Bulletin, v. 79, p. 429–458, https://doi.org/10.1130/0016-7606(1968)79[429:SOBINA]2.0.CO;2.

Armstrong, R.L., 1969, K-Ar dating of laccolith centers of the Colorado Plateau and vicinity: Geological Society of America Bulletin, v. 80, p. 2081–2086, https://doi.org/10.1130/0016-7606(1969)80[2081:KDOLCO]2.0.CO;2.

Armstrong, R.L., and Ward, P.L., 1993, Late Triassic to earliest Eocene magmatism in the North American Cordillera: Implications for the Western Interior Basin: Evolution of the western interior basin: Geological Association of Canada Special Paper 39, p. 49–72.

Arvizu, H.E., Iriondo, A., Izaguirre, A., Chavez-Cabello, G., Kamenov, G.D., Foster, D.A., Lozano-Santacruz, R., and Solis-Pichardo, G., 2009, Gneisses baneados paleoproterozoicos (1.76–1.73 Ga) de la zona Canteras-Puerto Penasco: Una nueva ocurrencia de rocas del basamento tipo Yavapai en el NW de Sonora, Mexico: Boletín de la Sociedad Geológica Mexicana, v. 61, p. 375–402.

Aubrey, W.M., 1992, New interpretations of the stratigraphy and sedimentology of uppermost Jurassic to lowermost Upper Cretaceous strata in the San Juan basin of northwestern New Mexico: U.S. Geological Survey Bulletin 1808-J, p. J1–J17.

Aubrey, W.M., 1996, Stratigraphic architecture and deformational history of Early Cretaceous foreland basin, eastern Utah and southwestern Colorado, *in* Huffman, A.C., Jr., Lund, W.R., and Godwin, L.H., eds., Geology and Resources of the Paradox Basin: Utah Geological Association, Guidebook 25, p. 211–220.

Ayers, W.B., Jr., Ambrose, W.A., and Yeh, J.S., 1994, Coalbed methane in the Fruitland Formation, San Juan Basin: depositional and structural controls on occurrence and resources, *in* Ayers, W.B., Jr., and Kaiser, W.R., eds., Coalbed Methane in the Cretaceous Fruitland Formation, San Juan Basin, New Mexico and Colorado: New Mexico Bureau of Mines and Mineral Resources Bulletin, v. 146, p. 13–61.

Baltz, E.H., 1967, Stratigraphy and regional tectonic implications of part of Upper Cretaceous and Tertiary rocks, east-central San Juan Basin, New Mexico: U.S. Geological Survey, Professional Paper 552, 101 p.

Barnes, H., Baltz, E.H., Jr., and Hayes, P.T., 1954, Geology and fuel resources of the Red Mesa area, La Plata and Archuleta counties, Colorado: U.S. Geological Survey Oil and Gas Investigations Map OM-149, scale 1:62,500.

Barth, A.P., and Wooden, J.L., 2006, Timing of magmatism following initial convergence at a passive margin, southwestern U.S. Cordillera, and ages of lower crustal magma sources: The Journal of Geology, v. 114, p. 231–245, https://doi.org/10.1086/499573.

Bauer, C.M., 1916, (1917), Stratigraphy of a part of the Chaco River valley: U.S. Geological Survey Professional Paper 98-P, p. 271–278.

Beard, L.S., Young, R.A., and Faulds, J.E., 2010, Structure, paleogeography, and extensional foundering of the Kingman uplift, northwestern Arizona and southwestern Nevada: Geological Society of America Abstracts with Programs, v. 42, no. 5, p. 75.

Bird, P., 1988, Formation of the Rocky Mountains, western United States: A continuum computer model: Science, v. 239, p. 1501–1507, https://doi.org/10.1126/science.239.4847.1501.

Blakey, R.C., 2012, Paleogeography and paleotectonics of Southwestern North America: Colorado Plateau Geosystems, DVD, Flagstaff, Arizona.

Blum, M., and Pecha, M., 2014, Mid-Cretaceous to Paleocene North American drainage reorganization from detrital zircons: Geology, v. 42, no. 7, p, 607–610, https://doi.org/10.1130/G35513.1.

Brister, B.S., and Chapin, C.E., 1994, Sedimentation and tectonics of the Laramide San Juan sag, southwestern Colorado: The Mountain Geologist, v. 31, no. 1, p. 2–18.

Busby-Spera, C.J., 1988, Speculative tectonic model for the early Mesozoic arc of the southwest Cordilleran United States: Geology, v. 16, p. 1121–1125, https://doi.org/10.1130/0091-7613(1988)016<1121:STMFTE>2.3.CO;2.

Bush, M.A., Horton, B.K., Murphy, M.A., and Stockli, D.F., 2016, Detrital record of initial basement exhumation along the Laramide deformation front, southern Rocky Mountains: Tectonics, v. 35, p. 2117–2130, https://doi.org/10.1002/2016TC004194.

Cather, S.M., 2003, Polyphase Laramide tectonism and sedimentation in the San Juan basin, New Mexico: New Mexico Geological Society Guidebook, 54th Field Conference, p. 119–132.

Cather, S.M., 2004, The Laramide orogeny in central and northern New Mexico and southern Colorado, *in* Mack, G.H., and Giles, K.A., eds., The Geology of New Mexico, A Geologic History: New Mexico Geological Society Special Publication 11, p. 203-248.

Cather, S.M., Chapin, C.E., and Kelley, S.A., 2012, Diachronous episodes off Cenozoic erosion in southwestern North America and their relationship to surface uplift, paleoclimate, paleodrainage, and paleoaltimetry: Geosphere, v. 8, p. 1177–1206, https://doi.org/10.1130/GES00801.1.

Chapin, C.E., 2012, Origin of the Colorado Mineral Belt: Geosphere, v. 8, p. 28–43, https://doi.org/10.1130/GES00694.1.

Chapin, C.E., Wilks, M., and McIntosh, W.C., 2004, Space-time patterns of Late Cretaceous to present magmatism in New Mexico—Comparison with Andean volcanism and potential for future volcanism, *in* Cather, S.M., et al., eds., Tectonics, Geochronology, and Volcanism in the Southern Rocky Mountains and Rio Grande Rift, New Mexico: New Mexico Bureau of Geology and Mineral Resources Bulletin 160, p. 13–40.

Coney, P.J., and Reynolds, S.J., 1977, Cordilleran Benioff zones: Nature, v. 270, p. 403–406, https://doi.org/10.1038/270403a0.

Craig, L.C., 1981, Lower Cretaceous rocks, southwestern Colorado and southeastern Utah, *in* Wiegand, D.L., ed., Geology of the Paradox Basin: Rocky Mountain Association of Geologists, p. 195–200.

Craig, L.C., Holmes, C.N., Cadigan, R.A., Freeman, V.L., Mullens, T.E., and Weir, G.W., 1955, Stratigraphy of the Morrison and related formations, Colorado Plateau region: A preliminary report: U.S. Geological Survey Bulletin 1009-E, p. 125–168.

Craigg, S.D., 2001, Geologic framework of the San Juan structural basin of New Mexico, Colorado, Arizona, and Utah with emphasis on Triassic through Tertiary rocks: U.S. Geological Survey Professional Paper 1420, 70 p.

Cumella, S.P., 1983, Relation of Upper Cretaceous regressive sandstone units of the San Juan Basin to source area tectonics, *in* Reynolds, M.W., and Dolly, E.D., eds., Mesozoic Paleogeography of West-Central United States: Rocky Mountain Section, SEPM (Society for Sedimentary Geology), p. 189–199.

Cunningham, C.G., Naeser, C.W., Marvin, R.F., Luedke, R.G., and Wallace, A.R., 1994, Ages of selected intrusive rocks and associated ore deposits in the Colorado Mineral Belt: U.S. Geological Survey Bulletin 2109, 31 p.

Currie, B.S., 1997, Sequence stratigraphy of nonmarine Jurassic-Cretaceous rocks, central Cordilleran foreland-basin system: Geological Society of America Bulletin, v. 109, p. 1206–1222, https://doi.org/10.1130/0016-7606(1997)109<1206:SSONJC>2.3.CO;2.

Currie, B.S., 1998, Upper Jurassic–Lower Cretaceous Morrison and Cedar Mountain Formations, NE Utah-NW Colorado: Relationships between nonmarine deposition and early Cordilleran foreland-basin development: Journal of Sedimentary Research, v. 68, p. 632–652, https://doi.org/10.2110/jsr.68.632.

Currie, B.S., 2002, Structural configuration of the Early Cretaceous Cordilleran foreland-basin system and Sevier thrust belt, Utah and Colorado: The Journal of Geology, v. 110, p. 697–718, https://doi.org/10.1086/342626.

Davis, S.J., Dickinson, W.R., Gehrels, G.E., Spencer, J.E., Lawton, T.F., and Carroll, A.R., 2010, The Paleogene California river: Evidence of Mojave-Uinta paleodrainage from U-Pb ages of detrital zircons: Geology, v. 38, no. 10, p. 931–934, https://doi.org/10.1130/G31250.1.

DeCelles, P.G., 2004, Late Jurassic to Eocene evolution of the Cordilleran thrust belt and foreland basin system, western U.S: American Journal of Science, v. 304, p. 105–168, https://doi.org/10.2475/ajs.304.2.105.

Dickinson, W.R., 2004, Evolution of the North American Cordillera: Annual Review of Earth and Planetary Sciences, v. 32, p. 13–45, https://doi.org/10.1146/annurev.earth.32.101802.120257.

Dickinson, W.R., 2011, The place of the Great Basin in the Cordilleran orogeny, *in* Steininger, R., and Pennell, B., eds., Great Basin Evolution and Metallogeny: Reno, Geological Society of Nevada 2010 Symposium, p. 419–436.

Dickinson, W.R., 2013, Rejection of the lake spillover model for initial incision of the Grand Canyon, and discussion of alternatives: Geosphere, v. 9, p. 1–20, https://doi.org/10.1130/GES00839.1.

Dickinson, W.R., and Gehrels, G.E., 2008, Sediment delivery to the Cordilleran foreland basin: Insights from U-Pb ages of detrital zircons in Upper Jurassic and Cretaceous strata of the Colorado Plateau: American Journal of Science, v. 308, p. 1041–1082, https://doi.org/10.2475/10.2008.01.

Dickinson, W.R., and Gehrels, G.E., 2009a, U-Pb ages of detrital zircons in Jurassic eolian and associated sandstones of the Colorado Plateau: Evidence for transcontinental dispersal and intraregional recycling of sediment: Geological Society of America Bulletin, v. 121, p. 408–433, https://doi.org/10.1130/B26406.1.

Dickinson, W.R., and Gehrels, G.E., 2009b, Use of U-Pb ages of detrital zircons to infer maximum depositional ages of strata: A test against a Colorado Plateau Mesozoic database: Earth and Planetary Science Letters, v. 288, no. 1–2, p. 115–125, https://doi.org/10.1016/j.epsl.2009.09.013.

Dickinson, W.R., and Lawton, T.F., 2001a, Carboniferous to Cretaceous assembly and fragmentation of Mexico: Geological Society of America Bulletin, v. 113, no. 9, p. 1142–1160, https://doi.org/10.1130/0016-7606(2001)113<1142:CTCAAF>2.0.CO;2.

Dickinson, W.R., and Lawton, T.F., 2001b, Tectonic setting and sandstone petrofacies of the Bisbee basin (USA-Mexico): Journal of South American Earth Sciences, v. 14, p. 475–504, https://doi.org/10.1016/S0895-9811(01)00046-3.

Dickinson, W.R., and Snyder, W.S., 1978, Plate tectonics of the Laramide Orogeny, *in* Matthews, V., ed., Laramide Folding Associated with Basement Block Faulting in the Western United States: Geological Society of America Memoir 151, p. 355–366, https://doi.org/10.1130/MEM151-p355.

Dickinson, W.R., Klute, M.A., Hayes, M.J., Janecke, S.U., Lundin, E.R., McKittrick, M.A., and Olivares, M.D., 1988, Paleogeographic and paleotectonic setting of Laramide sedimentary basins in the central Rocky Mountain region: Geological Society of America Bulletin, v. 100, p. 1023–1039, https://doi.org/10.1130/0016-7606(1988)100<1023:PAPSOL>2.3.CO;2.

Dickinson, W.R., Cather, S.M., and Gehrels, G.E., 2010, Detrital zircon evidence for derivation of arkosic sand in eolian Narbona Pass Member of the Eocene–Oligocene Chuska Sandstone from Precambrian basement rocks in central Arizona, *in* Fassett, J.E., Ziegler, K.E., and Lueth, V.W., eds., Geology of the Four Corners Country: New Mexico Geological Society 61st Annual Field Conference Guidebook, p. 125–134.

Dickinson, W.R., Lawton, T.F., Pecha, M., Davis, S.J., Gehrels, G.E., and Young, R.A., 2012, Provenance of the Paleogene Colton Formation (Uinta Basin) and Cretaceous–Paleogene provenance evolution in the Utah foreland: Evidence from U-Pb ages of detrital zircons, paleocurrent trends, and sandstone petrofacies: Geosphere, v. 8, no. 4, p. 854–880, https://doi.org/10.1130/GES00763.1.

Dilworth, O.L., 1960, Upper Cretaceous Farmington Sandstone of northwestern San Juan County, New Mexico [M.S. thesis]: Albuquerque, New Mexico University, 96 p.

Donahue, M.M., 2016, Episodic uplift of the Rocky Mountains: Evidence from U-Pb detrital zircon geochronology and low-temperature thermochronology with a chapter on using mobile technology for geoscience education [Ph.D. dissertation]: Albuquerque, University of New Mexico, UNM Digital Repository, 1177 p.

Ducea, M.N., 2001, The California arc: Thick granitic batholiths, eclogitic residues, lithospheric-scale thrusting, and magmatic flare-ups: GSA Today, v. 11, p. 4–10, https://doi.org/10.1130/1052-5173(2001)011<0004:TCATGB>2.0.CO;2.

Elston, D.P., and Young, R.A., 1991, Cretaceous-Eocene (Laramide) landscape development and Oligocene–Pliocene drainage reorganization of Transition Zone and Colorado Plateau, Arizona: Journal of Geophysical Research, v. 96, p. 12,389–12,406, https://doi.org/10.1029/90JB01978.

English, J.M., Johnston, S.T., and Wang, K., 2003, Thermal modeling of the Laramide orogeny: Testing the flat-slab subduction hypothesis: Earth and Planetary Science Letters, v. 214, no. 3–4, p. 619–632, https://doi.org/10.1016/S0012-821X(03)00399-6.

Epis, R.C., and Chapin, C.E., 1975, Geomorphic and tectonic implications of the post-Laramide, late Eocene erosion surface in the southern Rocky Mountains, *in* Curtis, B.F., ed., Cenozoic History of the Southern Rocky Mountains: Geological Society of America Memoir 144, p. 45–74, https://doi.org/10.1130/MEM144-p45.

Erpenbeck, M.F., 1979, Stratigraphic relationships and depositional environments of the Upper Cretaceous Pictured Cliffs Sandstone and Fruitland Formation, southwestern San Juan Basin, New Mexico [M.S. thesis]: Lubbock, Texas, Texas Tech University, 78 p.

Evanoff, E., and Chapin, C.E., 1994, Composite nature of the "late Eocene surface" of the Front Range and adjacent regions, Colorado and Wyoming: Geological Society of America Abstracts with Programs, v. 26, p. 12.

Fassett, J.E., 1985, Early Tertiary paleogeography and paleotectonics of the San Juan Basin area, New Mexico and Colorado, *in* Flores, R.M., and Kaplan, S.S., eds., Cenozoic Paleogeography of the West-Central United States: Denver, Rocky Mountain Section, Society of Economic Paleontologists and Mineralogists, p. 317–334.

Fassett, J.E., 2009, Geology and coal resources of the Upper Cretaceous Fruitland Formation, San Juan basin, New Mexico and Colorado, *in* Kirschbaum, M.A., Roberts, L.N.R., and Biewick, L.R.H., Geologic Assessment of Coal in the Colorado Plateau, Arizona, Colorado, New Mexico, Utah: U.S. Geological Survey Professional Paper 1625-B, p. 1–77.

Fassett, J.E., and Hinds, J.S., 1971, Geology and Fuel Resources of the Fruitland Formation and Kirtland Shale of the San Juan Basin, New Mexico and Colorado: U.S. Geological Survey Professional Paper 676, 76 p.

Fassett, J.E., and Steiner, M.B., 1997, Precise age of C33N–C32R magnetic polarity reversal, San Juan Basin, New Mexico and Colorado: New Mexico Geological Society, 48th Field Conference Guidebook, p. 239–247.

Fassett, J.E., Heizler, M.T., and McIntosh, W.C., 2010, Geologic implications of an $^{40}Ar/^{39}Ar$ single-crystal sanidine age for an altered volcanic ash bed in the Paleocene Nacimiento Formation in the southern San Juan Basin, *in* Fassett, J.E., Ziegler, K.E., and Lueth, V.W., eds., Geology of the Four Corners Country: New Mexico Geological Society 61st Annual Field Conference Guidebook, p. 147–156.

Favorito, D.A., and Seedorff, E., 2017, Chracterization and reconstruction of Laramide shortening and superimposed Cenozoic extension, Romero Wash-Tecolote Ranch area, southeastern Arizona: Geosphere, v. 13, p. 577–607, https://doi.org/10.1130/GES01381.1.

Feldman, J., 2010, The emplacement and exhumation history of the Twin Lakes batholith and implications for the Laramide orogeny and flat slab subduction [M.S. thesis]: Socorro, New Mexico Institute of Mining and Technology, 174 p.

Flores, R.M., and Erpenbeck, M.F., 1981, Differentiation of delta front and barrier lithofacies of the Upper Cretaceous Pictured Cliffs Sandstone, southwestern San Juan Basin, New Mexico: The Mountain Geologist, v. 18, no. 2, p. 23–34.

Gehrels, G., and Pecha, M., 2014, Detrital zircon U-Pb geochronology and Hf isotope geochemistry of Paleozoic and Triassic passive margin strata of western North America: Geosphere, v. 10, no. 1, p. 49–65, https://doi.org/10.1130/GES00889.1.

Gehrels, G.E., Valencia, V., and Pullen, A., 2006, Detrital zircon geochronology by laser-ablation multicollector ICP-MS at the Arizona LaserChron Center, *in* Loszewski, T., and Huff, W., eds., Geochronology: Emerging Opportunities, Paleontology Society Short Course: Paleontology Society Papers, v. 11, 10 p.

Gehrels, G.E., Valencia, V., and Ruiz, J., 2008, Enhanced precision, accuracy, efficiency, and spatial resolution of U-Pb ages by laser ablation–multicollector–inductively coupled plasma–mass spectrometry: Geochemistry Geophysics Geosystems, v. 9, Q03017, https://doi.org/10.1029/2007GC001805.

Gehrels, G.E., Blakey, R., Karlstrom, K.E., Timmons, J.M., Dickinson, B., and Pecha, M., 2011, Detrital zircon U-Pb geochronology of Paleozoic strata in the Grand Canyon, Arizona: Lithosphere, v. 3, no. 3, p. 183–200, https://doi.org/10.1130/L121.1.

Goldstrand, P.M., 1994, Tectonic development of Upper Cretaceous to Eocene strata of southwestern Utah: Geological Society of America Bulletin, v. 106, p. 145–154, https://doi.org/10.1130/0016-7606(1994)106<0145:TDOUCT>2.3.CO;2.

Gonzales, D.A., 2010, The enigmatic Late Cretaceous McDermott Formation: New Mexico Geological Society Guidebook, 61st Field Conference, Geology of the Four Corners Country, 2010, p. 157–162.

Gonzales, D.A., 2015, New U-Pb zircon and $^{40}Ar/^{39}Ar$ age constraints on the Late Mesozoic to Cenozoic plutonic record in the Western San Juan Mountains: The Mountain Geologist, v. 52, no. 2, p. 5–42.

González-León, C.M., Solari, L., Sole, J., Ducea, M.N., Lawton, T.F., Bernal, J.P., Becuar, E.G., Gray, F., Martinez, M.L., and Santacruz, R.L., 2011, Stratigraphy, geochronology, and geochemistry of the Laramide magmatic arc in north-central Sonora, Mexico: Geosphere, v. 7, no. 6, p. 1392–1418, https://doi.org/10.1130/GES00679.1.

Gradstein, F.M., Ogg, J.G., Schmitz, M., and Ogg, G., eds., 2012, The Geologic Time Scale 2012: Oxford, UK, Elsevier.

Harris, D.R., 1980, Exhumed paleochannels in the Lower Cretaceous Cedar Mountain Formation near Green River, Utah: Brigham Young University Geology Studies, v. 27, p. 51–66.

Haxel, G.B., Anderson, T.H., Briskey, J.A., Tosdal, R.M., Wright, J.E., and May, D.J., 2008, Late Jurassic igneous rocks in south-central Arizona and north-central Sonora: Magmatic accompaniment of crustal extension, *in* Spencer, J.E., and Titley, S.R., eds., Ores and Orogenesis: Circum-Pacific Tectonics, Geologic Evolution, and Ore Deposits: Tucson, Arizona Geological Society Digest 22, p. 333–335.

Heller, P.L., Mathers, G., Dueker, K., and Foreman, B., 2013, Far-traveled latest Cretaceous–Paleocene conglomerates of the Southern Rocky Mountains, USA: Record of transient Laramide tectonism: Geological Society of America Bulletin, v. 125, no. 3/4, p. 490–498, https://doi.org/10.1130/B30699.1.

Hoffman, P.F., 1988, Early Proterozoic assembly and growth of Laurentia: Annual Review of Earth and Planetary Sciences, v. 16, p. 543–603, https://doi.org/10.1146/annurev.ea.16.050188.002551.

Hunt, A.P., 1984, Stratigraphy, sedimentology, taphonomy and magnetostratigraphy of the Fossil Forest are, San Juan County, New Mexico [M.S. thesis]: Socorro, New Mexico Institute of Mining and Technology, 338 p.

Hunt, A.P., and Lucas, S.G., 1992, Stratigraphy, paleontology, and age of the Fruitland and Kirtland Formations (Upper Cretaceous), San Juan basin, New Mexico, *in* Lucas, S.G., Kues, B.S., Williamson, T.E., and Hunt, A.P., eds., San Juan Basin IV: Socorro, New Mexico Geological Society Guidebook, 43rd Annual Field Conference, p. 217–240.

Johnson, H.D., Krevitzky, R.M., Link, P.K., and Biek, R.F., 2011, Detrital zircons from the Late Cretaceous middle member Grand Castle Formation, south-central Utah: Recycled Mesozoic eolianites: Geological Society of America Abstracts with Programs, v. 43, no. 4, p. 68.

Jordan, T.E., 1981, Thrust loads and foreland basin evolution, Cretaceous, western United States: The American Association of Petroleum Geologists Bulletin, v. 65, p. 2506–2520.

Karlstrom, K.E., Lee, J., Kelley, S., Crow, R., Crossey, L.J., Young, R., Lazear, G., Beard, L.S., Ricketts, J., Fox, M., and Shuster, D., 2014, Formation of the Grand Canyon 5 to 6 million years ago through integration of older palaeocanyons [with Supplementary materials]: Nature Geoscience, v. 7, p. 239–244, https://doi.org/10.1038/ngeo2065.

Kelley, V.C., 1950, Precambrian rocks of the San Juan Basin, *in* Kelley, V.C., Beaumont, E.C., and Silver, C., San Juan Basin, New Mexico and Colorado: New Mexico Geological Society, First Annual Fall Field Conference Guidebook, p. 53–55.

Kelley, V.C., 1951, Tectonics of the San Juan Basin, *in* Smith, C.T., and Silver, C., eds., San Juan Basin (New Mexico and Arizona): New Mexico Geological Society, Second Annual Fall Field Conference Guidebook, p. 124–131.

Kelley, V.C., 1955, Regional Tectonics of the Colorado Plateau and Relationship to the Origin and Distribution of Uranium: University of New Mexico Publications in Geology 5, 120 p.

Kelley, V.C., 1957, Tectonics of the San Juan Basin and surrounding areas, *in* Little, C.J., and Gill, J.J., eds., Geology of Southwestern San Juan Basin: Four Corners Geological Society, 2nd Field Conference Guidebook, p. 44–52.

Kirkland, J.I., and Madsen, S.K., 2007, The Lower Cretaceous Cedar Mountain Formation, eastern Utah: St. George, Utah, Geological Society of America Annual Meeting, 108 p.

Klute, M.A., 1986, Sedimentology and sandstone petrography of the upper Kirtland Shale and Ojo Alamo Sandstone, Cretaceous–Tertiary boundary, western and southern San Juan Basin, New Mexico: American Journal of Science, v. 286, p. 463–488, https://doi.org/10.2475/ajs.286.6.463.

Kottlowski, F.E., 1957, Mesozoic strata flanking the southwestern San Juan Mountains, Colorado and New Mexico: New Mexico Geological Society, 8th Field Conference Guidebook, p. 138–153.

Larsen, J.S., Link, P.K., Roberts, E.M., Tapanila, L., and Fanning, C.M., 2010, Cyclic stratigraphy of the Paleogene Pine Hollow Formation and detrital zircon provenance of Campanian to Eocene sandstones of the Kaiparowits and Table Cliffs basins, south-central Utah, *in* Carney, S.M., Tabet, D.E., and Johnson, C.L., eds., Geology of South-Central Utah: Utah Geological Association Publication 39, p. 194–224.

Laskowski, A.K., DeCelles, P.G., and Gehrels, G.E., 2013, Detrital zircon geochronology of Cordilleran retroarc foreland basin strata, western North America: Tectonics, v. 32, no. 5, p. 1027–1048, https://doi.org/10.1002/tect.20065.

Lawton, T.F., 1986, Fluvial systems of the Upper Cretaceous Mesaverde Group and Paleocene North Horn Formation, central Utah: a record of transition from thin-skinned to thick-skinned deformation in the foreland region, *in* Peterson, J.A., ed., Paleotectonics and Sedimentation in the Rocky Mountain Region, United States: American Association of Petroleum Geologists Memoir 41, p. 423–442.

Lawton, T.F., 2004, Upper Jurassic and Lower Cretaceous strata of southwestern New Mexico and northern Chihuahua, Mexico, *in* Mack, G.H., and Giles, K.A., eds., The Geology of New Mexico: A Geologic History: New Mexico Geological Society Special Publication 11, p. 153–168.

Lawton, T.F., 2008, Laramide sedimentary basins, *in* Miall, A.D., ed., The Sedimentary Basins of the United States and Canada: Amsterdam, Elsevier, p. 429–450, https://doi.org/10.1016/S1874-5997(08)00012-9.

Lawton, T.F., and Bradford, B.A., 2011, Correlation and provenance of Upper Cretaceous (Campanian) fluvial strata in the Cordilleran foreland basin, Utah, from zircon U-Pb geochronology and petrography: Journal of Sedimentary Research, v. 81, no. 7, p. 495–512, https://doi.org/10.2110/jsr.2011.45.

Lawton, T.F., and McMillan, N.J., 1999, Arc abandonment as a cause for passive continental rifting: Comparison of the Jurassic Mexican Borderland rift and the Cenozoic Rio Grande rift: Geology, v. 27, p. 779–782, https://doi.org/10.1130/0091-7613(1999)027<0779:AAAACF>2.3.CO;2.

Lazear, G., Karlstrom, K.E., Aslan, A., and Kelley, S., 2013, Denudation and flexural isostatic response of the Colorado Plateau and southern Rocky Mountain region since 10 Ma: Geosphere, v. 9, p. 792–814, https://doi.org/10.1130/GES00836.1.

Lehman, T.M., 1985, Depositional environments of the Naashoibito Member of the Kirtland Shale, Upper Cretaceous, San Juan Basin, New Mexico, *in* Wolberg, D.L., compiler, Contributions to Late Cretaceous Paleontology and Stratigraphy of New Mexico: New Mexico Bureau of Mines and Mineral Resources, Circular 195, p. 55–79.

Leier, A.L., and Gehrels, G.E., 2011, Continental-scale detrital zircon provenance signatures in Lower Cretaceous strata, western North America: Geology, v. 39, p. 399–402, https://doi.org/10.1130/G31762.1.

Leveille, R.A., and Stegen, R.J., 2012, The southwestern North America Porphyry Copper Province, *in* Hedenquist, J.W., Harris, M., and Camus, F., eds., Geology and Genesis of Major Copper Deposits and Districts of the World: A Tribute to Richard H. Sillitoe: Society of Economic Geologists Special Publication, v. 16, p. 361–401.

Liu, L., Gurnis, M., Seton, M., Saleeby, J., Muller, R.D., and Jackson, J.M., 2010, The role of oceanic plateau subduction in the Laramide orogeny: Nature Geoscience, v. 3, p. 353–357, https://doi.org/10.1038/ngeo829.

Lorraine, M.M., and Gonzales, D.A., 2003, Lahars or not lahars?: An evaluation of the volcanic connection for the late Cretaceous McDermott Formation near Durango, Colorado: Geological Society of America, Rocky Mountain Section, 55th Annual Meeting, abstract no 13-3.

Lucas, S.G., 2004, The Triassic and Jurassic systems in New Mexico, *in* Mack, G.H., and Giles, K.A., eds., The Geology of New Mexico: A Geologic History: New Mexico Geological Society Special Publication 11, p. 137–152.

Ludvigson, G.A., Joeckel, R.M., Gonzalez, L.A., Gulbranson, E.L., Rasbury, E.T., Hunt, G.J., Kirkland, J.I., and Madsen, S., 2010, Correlation of Aptian–Albian carbonate isotope excursions in continental strata of the Cretaceous foreland basin, eastern Utah, U.S.A: Journal of Sedimentary Research, v. 80, p. 955–974, https://doi.org/10.2110/jsr.2010.086.

Ludwig, K.R., 2008, Isoplot 3.60: Berkeley Geochronology Center, Special Publication No. 4, 77 p.

McCormick, W.L., 1950, A study of the McDermott Formation, Upper Cretaceous age in the San Juan basin, southwestern Colorado and northern New Mexico [M.S. thesis]: Urbana, Illinois, University of Illinois, 51 p.

Miller, D.M., Nilsen, T.H., and Bilodeau, W.L., 1992, Late Cretaceous to early Eocene geologic evolution of the U.S. Cordillera, *in* Burchfiel, B.C., Lipman, P.W., and Zoback, M.L., eds., The Cordilleran Orogen: Conterminous U.S.: Geological Society of America, The Geology of North America, v. G-3, p. 205–260.

Mizer, J.D., 2013, Uranium-lead geochronology of magmatism in the Central Mining District, New Mexico [M.S. thesis]: Tucson, Arizona, University of Arizona, 57 p.

Molenaar, C.M., 1977, Stratigraphy and depositional history of Upper Cretaceous rocks of the San Juan basin area, New Mexico and Colorado, with a note on economic reserves, *in* Fassett, J.E., ed., San Juan Basin III, Northwestern New Mexico: New Mexico Geological Society 28th Field Conference, p. 159–166.

Molenaar, C.M., 1983, Major depositional cycles and regional correlations of Upper Cretaceous rocks, southern Colorado Plateau and adjacent areas, *in* Reynolds, M.W., and Dolly, E.D., eds., Mesozoic Paleogeography of the West-Central United States: Rocky Mountain Section, SEPM (Society for Sedimentary Geology) Rocky Mountain Paleogeography Symposium 2, p. 201–224.

Mutschler, F.E., Larson, E.E., and Ross, M.L., 1997, Potential for alkaline igneous rock-related gold deposits in the Colorado Plateau laccolithic centers, *in* Friedman, J.D., and Huffman, A.C., Jr., eds., Laccolith Complexes of Southeastern Utah: Time of Emplacement and Tectonic Setting—Workshop Proceedings: U.S. Geological Survey Bulletin 2158, p. 233–252.

New Mexico Bureau of Geology and Mineral Resources, 2003, Geologic map of New Mexico, 1:500,000: New Mexico Bureau of Geology and Mineral Resources.

Nummedal, D., 2004, Tectonic and eustatic controls on Upper Cretaceous stratigraphy of New Mexico, *in* Mack, G.H., and Giles, K.A., eds., The Geology of New Mexico; A Geologic History: New Mexico Geological Society Special Publication 11, p. 169–182.

O'Shea, C., 2009, Volcanic influence over fluvial sedimentation in the Cretaceous McDermott Member, Animas Formation, southwestern Colorado [M.S. thesis]: Bowling Green, Ohio, Bowling Green State University, 90 p.

Pappe, D.J., Heizler, M.T., Williamson, T.E., Masson, I.P., Brusatte, S., Weil, A., and Secord, R., 2013, New age constraints on the Late Cretaceous through Early Paleogene rocks in the San Juan basin, New Mexico: Geological Society of America Abstracts with Programs, v. 45, no. 7, p. 290.

Pazzaglia, F., and Kelley, S., 1998, Large-scale geomorphology and fission-track thermochronology in topographic and exhumation reconstructions of the southern Rocky Mountains: Rocky Mountain Geology, v. 33, no. 2, p. 229–257, https://doi.org/10.2113/33.2.229.

Pederson, J.L., Mackley, R.D., and Eddleman, J.L., 2002, Colorado Plateau uplift and erosion evaluated using GIS: GSA Today, v. 12, no. 8, p. 4–10, https://doi.org/10.1130/1052-5173(2002)012<0004:CPUAEE>2.0.CO;2.

Peterson, F., 1984, Fluvial sedimentation on a quivering craton: Influence of slight crustal movements on fluvial processes, Upper Jurassic Morrison Formation, western Colorado Plateau: Sedimentary Geology, v. 38, p. 21–49, https://doi.org/10.1016/0037-0738(84)90073-3.

Powell, J.S., 1972, The Gallegos Sandstone (formerly Ojo Alamo Sandstone) of the San Juan basin, New Mexico [M.S. thesis]: Tucson, Arizona, University of Arizona, 131 p.

Pullen, A., Ibanez-Mejia, M., Gehrels, G.E., Ibanez-Mejia, J.C., and Pecha, M., 2014, What happens when n=1000?: Creating large-n geochronological datasets with LA-ICP-MS for geological investigations: Journal of Analytical Atomic Spectrometry, v. 29, p. 971–980, https://doi.org/10.1039/C4JA00024B.

Ramos-Velázquez, E., Calmus, T., Valencia, V., Iriondo, A., Valencia-Moreno, M., and Bellon, H., 2008, U-Pb and $^{40}Ar/^{39}Ar$ geochronology of the coastal Sonora batholith, New insights on Laramide continental arc magmatism: Revista Mexicana de Ciencias Geologicas, v. 25, no. 2, p. 314–333.

Reeside, J.B., Jr., 1924, Upper Cretaceous and Tertiary Formations of the western part of the San Juan basin, Colorado and New Mexico: U.S. Geological Survey Professional Paper 134, 70 p.

Robinson, J.W., and McCabe, P.J., 1998, Evolution of a braded river system: The Salt Wash Member of the Morrison Formation (Jurassic) in southern Utah, *in* Shanley, K.W., and McCabe, P.J., eds., Relative Role of Eustasy, Climate, and Tectonism in Continental Rocks: SEPM (So-

ciety of Sedimentary Geology) Special Publication No. 59, p. 93–107, https://doi.org/10.2110/pec.98.59.0093.
Ross, G.M., and Parrish, R.R., 1991, Detrital zircon geochronology of metasedimentary rocks in the southern Omineca Belt, Canadian Cordillera: Canadian Journal of Earth Sciences, v. 28, p. 1254–1270, https://doi.org/10.1139/e91-112.
Saleeby, J.B., 2003, Segmentation of the Laramide slab—evidence from the southern Sierra Nevada region: Geological Society of America Bulletin, v. 115, no. 6, p. 655–668, https://doi.org/10.1130/0016-7606(2003)115<0655:SOTLSF>2.0.CO;2.
Seedorff, E., Barton, M.D., Gehrels, G.E., Johnson, D.A., Maher, D.J., Stavast, W.J.A., and Flesch, E., 2005, Implications of new U-Pb dates from porphyry copper-related plutons in the Superior-Globe-Ray-Christmas area, Arizona: Geological Society of America Abstracts with Programs, v. 37, no. 7, p. 164, paper no. 65-11.
Semken, S.C., and McIntosh, W.C., 1997, $^{40}Ar/^{39}Ar$ age determinations for the Carrizo Mountains laccolith, Navajo Nation, Arizona, *in* Anderson, O.J., Kues, B.S., and Lucas, S.G., eds., Mesozoic Geology and Paleontology of the Four Corners Region: New Mexico Geological Society 48th Annual Field Conference, p. 75–80.
Sharman, G.R., Covault, J.A., Stockli, D.F., Wroblewski, A.F.-J., and Bush, M.A., 2017, Early Cenozoic drainage reorganization of the United States Western Interior–Gulf of Mexico sediment routing system: Geology, v. 45, no. 2, p. 187–190, https://doi.org/10.1130/G38765.1.
Sikkink, P.G.L., 1987, Lithofacies relationships and depositional environment of the Tertiary Ojo Alamo Sandstone and related strata, San Juan basin, New Mexico and Colorado, *in* Fassett, J.E., and Rigby, J.K., Jr., eds., The Cretaceous–Tertiary Boundary in the San Juan and Raton Basins, New Mexico and Colorado: Geological Society of America Special Paper 209, p. 81–104, https://doi.org/10.1130/SPE209-p81.
Simpson, G.G., 1948, The Eocene of the San Juan basin, New Mexico: American Journal of Science, v. 246, pt. 1, p. 275–282; pt. 2, p. 363–385.
Smith, L.N., 1988, Basin analysis of the lower Eocene San Jose Formation, San Juan Basin, New Mexico and Colorado [Ph.D. dissertation]: Albuquerque, University of New Mexico, 166 p.
Smith, L.N., 1992, Stratigraphy, sediment dispersal and paleogeography of the Lower Eocene San Jose Formation, San Juan basin, New Mexico and Colorado, *in* Lucas, S.G., Kues, B.S., Williamson, T.E., and Hunt, A.P., eds., San Juan Basin IV: New Mexico Geological Society, 43rd Field Conference, p. 297–309.
Smith, L.N., Lucas, S.G., and Elston, W.E., 1985, Paleocene stratigraphy, sedimentation and volcanism of New Mexico, *in* Flores, R.M., and Kaplan, S.S., eds., Cenozoic Paleogeography of the West-Central United States: Rocky Mountain Section, SEPM (Society for Sedimentary Geology), p. 293–315.
Sullivan, R.M., and Lucas, S.G., 2006, The Kirtlandian land vertebrate "age"—Faunal composition, temporal position and biostratigraphic correlation in the nonmarine Upper Cretaceous of western North America, *in* Lucas, S.G., and Sullivan, R.M., eds., Late Cretaceous Vertebrates from the Western Interior: New Mexico Museum of Natural History and Science Bulletin, v. 35, p. 7–29.
Surpless, K.D., Graham, S.A., Covault, J.A., and Wooden, J.L., 2006, Does the Great Valley Group contain Jurassic strata?: Reevaluation of the age and early evolution of a classic foreland basin: Geology, v. 34, no. 1, p. 21–24, https://doi.org/10.1130/G21940.1.
Torres, R., Ruiz, J., Patchett, P.J., and Grajales, J.M., 1999, A Permo-Triassic arc in eastern Mexico: Tectonic implications for reconstructions of southern North America, *in* Batolini, C., Wilson, J.L., and Lawton, T.F., eds., Mesozoic Sedimentary and Tectonic History of North-Central Mexico: Geological Society of America Special Paper 340, p. 191–196, https://doi.org/10.1130/0-8137-2340-X.191.
Tschudy, R.H., Tschudy, B.D., and Craig, L.C., 1984, Palynological evaluation of Cedar Mountain and Burro Canyon Formations, Colorado Plateau: U.S. Geological Survey Professional Paper 1281, 24 p.
Valencia, V.A., Ruiz, J., Barra, F., Gehrels, G., Ducea, M., Titley, S.R., Ochoa-Landin, L., 2005, U-Pb zircon and Re-Os molybdenite geochronology from La Caridad porphyry copper deposit: Insights for the duration of magmatism and mineralization in the Nacozari District, Sonora, Mexico: Mineralium Deposita, v. 40, p. 175–191.
Valencia, V.A., Noguez-Alcantara, B., Barra, F., Ruiz, J., Gehrels, G., Quintanar, F., and Valencia-Moreno, M., 2006, Re-Os molybdenite and LA-ICPMS-MC U-Pb zircon geochronology for the Milpillas porphyry copper deposit: Insights for the timing of mineralization in the Cananea District, Sonora, Mexico: Revista Mexicana de Ciencias Geológicas, v. 23, no. 1, p. 39–53.
Vickre, P.G., Graybeal, F.T., Fleck, R.J., Barton, M.D., and Seedorff, E., 2014, Succession of Laramide magmatic and magmatic-hydrothermal events in the Patagonia Mountains, Santa Cruz County, Arizona: Economic Geology and the Bulletin of the Society of Economic Geologists, v. 109, p. 1667–1704, https://doi.org/10.2113/econgeo.109.6.1667.
Walker, J.D., and Geissman, J.W., compilers, 2009, Geologic Time Scale: Geological Society of America, https://doi.org/10.1130/2009.CTS004R2C.
Wernicke, B., 2011, The California River and its role in carving Grand Canyon: Geological Society of America Bulletin, v. 123, no. 7–8, p. 1288–1316, https://doi.org/10.1130/B30274.1.
Wilson, R.F., 1967, Chapter III, conclusions and symposium hypothesis, *in* McKee, E.D., Wilson, R.F, Breed, W.J., and Breed, C.S., eds., Evolution of the Colorado River in Arizona: Museum of Northern Arizona Bulletin, no. 44, p. 46–61.
Yonkee, W.A., and Weil, A.B., 2015, Tectonic evolution of the Sevier and Laramide belts within the North American Cordillera orogenic system: Earth-Science Reviews, v. 150, p. 531–593, https://doi.org/10.1016/j.earscirev.2015.08.001.
Young, R.A., and McKee, E.H., 1978, Early and middle Cenozoic drainage and erosion in west-central Arizona: Geological Society of America Bulletin, v. 89, no. 12, p. 1745–1750, https://doi.org/10.1130/0016-7606(1978)89<1745:EAMCDA>2.0.CO;2.